incubation, which was relatively slow compared with cM362-99 (Supplementary Fig. 4). These results suggested that the length of dsRNA together with the presence of cM362 influences the internalization speed and retention time in the TLR3-situated early endosome.

The abilities of cM362-dsRNAs to induce cytokine production were then examined using splenic DCs from wild-type and TLR3-deficient mice. cM362-79 and -139 induced a slight increase in TNF-α and IL-6 production by splenic CD11c$^+$ DCs in a TLR3-dependent manner (Supplementary Fig. 5a). Again, cM362-dsRNAs did not activate cytoplasmic RNA sensors in mouse splenic CD11c$^+$ DCs (Supplementary Fig. 5b). Thus, the chimeric compound cM362-139 appears to possess novel features that enable it to be quickly delivered to TLR3-positive endosomes, retained for a long period in the endosomes, and activate TLR3 but not RIG-like receptor (RLR).

As a TLR3-specific agonist with high activity, we selected cM362-139 for further *in vivo* studies with tumour-loaded mice.

Chemical synthesis of cM362-140. As chemical synthesis of sODN-dsRNA is indispensable for complying with good manufacturing practice (GMP) criteria, we started trials for chemical synthesis of cM362-140 (Fig. 1a), and its activity was analysed in comparison with *in vitro* transcribed cM362-139 (Fig. 1a,b). A synthesized 165 mer sense cM362-RNA hybrid and a 140mer antisense RNA, both of which consisted of single bands on 8% polyacrylamide gel electrophoresis (PAGE) and high-performance liquid chromatography/mass spectrometry analysis were annealed to make cM362-140 (Fig. 1a, lower panel). First, the degradability of cM362-139(IVT) and chemically synthesized cM362-140 were tested under different conditions. Both compounds were stable during incubation in PBS with or without 10% FBS, mouse serum or human serum at 37 °C for 60 min. cM362-139(IVT) was slightly degraded in PBS containing FBS or mouse serum but not human serum during incubation at 42 °C (Fig. 1c). Notably, cM362-139(IVT) was susceptible to degradation by nucleases during incubation in RNase-free water containing 10% FBS or mouse serum, but relatively resistant to human serum (Supplementary Fig. 6). In contrast, cM362-140 was quite stable under all these conditions. Thus, synthetic cM362-140 consisting of the cM362-capped RNA strand and antisense RNA strand was found to be more resistant to serum nucleases than cM362-139(IVT) consisting of three nucleotide strands.

cM362-140 activates TLR3 but not cytoplasmic RNA sensors. cM362-140 efficiently induced TLR3-dependent IFN-β promoter activation similar to cM362-139(IVT), when it was used to stimulate HEK293 cells expressing human TLR3 by simple addition or endosomal delivery (Fig. 2a, left and centre panels). Activation of cytoplasmic RNA/DNA sensors by cM362-140 was hardly observed in HEK293 cells similar to cM362-139(IVT) (Fig. 2a, right panel). To address the potential of cM362-140 for cytokine induction, splenic DCs from wild-type, *Tlr3*$^{-/-}$ or *Mavs*$^{-/-}$ mice were stimulated with poly(I:C), cM362-139(IVT), control synthetic dsRNA140 or cM362-140, either alone or complexed with N-(1-(2,3-Dioleoyloxy)propyl)-N, N, N-trimethylammonium methyl-sulfate) (DOTAP) to deliver them to endosomes, or complexed with Lipofectamine to deliver them to cytoplasm. Extracellular addition of cM362-139(IVT) and cM362-140 to splenic DCs induced a subtle increase in TNF-α, IL-6 and IFN-β production compared with poly(I:C) treatment, whereas synthetic dsRNA140 (with no GpC) did not induce any cytokine over the detection limits (Fig. 2b, left panels). Endosomal delivery of cM362-139(IVT) or cM362-140 with DOTAP also induced minimal levels of TNF-α, IL-6 and IFN-β dependent upon TLR3 (Fig. 2b, centre panels). When the compounds were transfected into cytoplasm with Lipofectamine, MAVS-dependent cytokine production was barely observed with cM362-140, whereas only low levels of IL-6 and IFN-β were induced with cM362-139 in TLR3 KO DC (Fig. 2b, right panel). This MAVS activity may reflect the exposure of a few 5′-triphosphated species of cM362-139(IVT) due to minor RNA degradation. These results indicate that cM362-140 targets endosomal TLR3 and activate the TICAM-1 pathway in both human and mouse cells.

***In vivo* cytokine induction by cM362-140.** Injection of poly(I:C) into mouse peritoneal cavity strongly induced proinflammatory cytokine production in a TLR3-independent manner and high level of TNF-α and IL-6 were detected in sera at 3 h after injection (Fig. 3a). In contrast, both cM362-140 and cM362-139(IVT) hardly induced cytokine production and serum TNF-α, IL-6 and IL-10 levels were very low, which is mediated by TLR3 (Fig. 3a). Unlike poly(I:C), cM362-140 or -139(IVT) induced undetectable levels of IFN-β in wild-type mouse sera (Supplementary Fig. 7).

A subcutaneous (s.c.) injection of cM362-140 induced the mRNAs of IFN-β and IL-6, but not TNF-α, in the inguinal and axillary lymph nodes (LNs) and spleen; the expression level was lower than that induced by poly(I:C) (Fig. 3b). These results suggest that TLR3-specific activation with cM362-140 results in low levels of cytokine production *in vivo* either by intraperitoneal (i.p.) or s.c. administration.

EG7 tumour regression by CTL induced by cM362-139/140. The next question was whether cM362-139(IVT) causes tumour growth retardation as observed with poly(I:C). EG7 cells (a lymphoma cell line containing ovalbumin, OVA) were inoculated into the back of wild-type (WT) C57BL/6 mice, and the indicated materials were injected s.c. around the EG7 tumour that developed (Fig. 4). Tumour growth was mildly retarded by treatment with poly(I:C) or cM362-139(IVT) alone (Fig. 4a). Combination therapy of OVA and poly(I:C) or cM362-139(IVT) resulted in complete remission of EG7 tumour >12 days after the treatment (Fig. 4a). The results infer that the combination of RNA adjuvant + tumour Ag exerts antitumour immune effect in spite of the low induction of proinflammatory cytokines.

We next tested whether s.c. injection of cM362-139(IVT) plus OVA induced CTL proliferation. The OVA tetramer assay and IFN-γ production were employed to evaluate OVA-specific CD8$^+$ T-cell activation. Combination therapy of cM362-139(IVT) with OVA exhibited an increase in the frequency of Ag-specific CD8$^+$ T cells comparable to poly(I:C) with OVA (Fig. 4b). Ag-specific CD8$^+$ T cells clonally proliferated against EG7 as *in vitro* cytotoxicity was directed exclusively to EG7 in mice stimulated with cM362-139(IVT) with OVA (Fig. 4c) as well as poly(I:C) with OVA[9]. EG7 growth retardation by cM362-139(IVT) with OVA was largely abrogated in TLR3 KO mice (Supplementary Fig. 8), suggesting that cM362-139(IVT) acts on host TLR3 *in vivo*. However, mild tumour growth retardation was still observed with cM362-139(IVT) with OVA in TLR3 KO mice (Supplementary Fig. 8), implying minor involvement of EG7 cell TLR3 or other host RNA sensors, such as RLR[26] and DEAD-box helicases[27], in *in vivo* tumour regression. Yet, tumor cell's TLR3 signaling and chemokine induction might affect tumor remission (refs 28–30).

We finally tested whether chemically synthesized cM362-140 harbours the ability to retard EG7 growth in the same model. The synthetic cM362-140 showed ~80% activity for IFN-β reporter activation compared with cM362-139(IVT) and a single

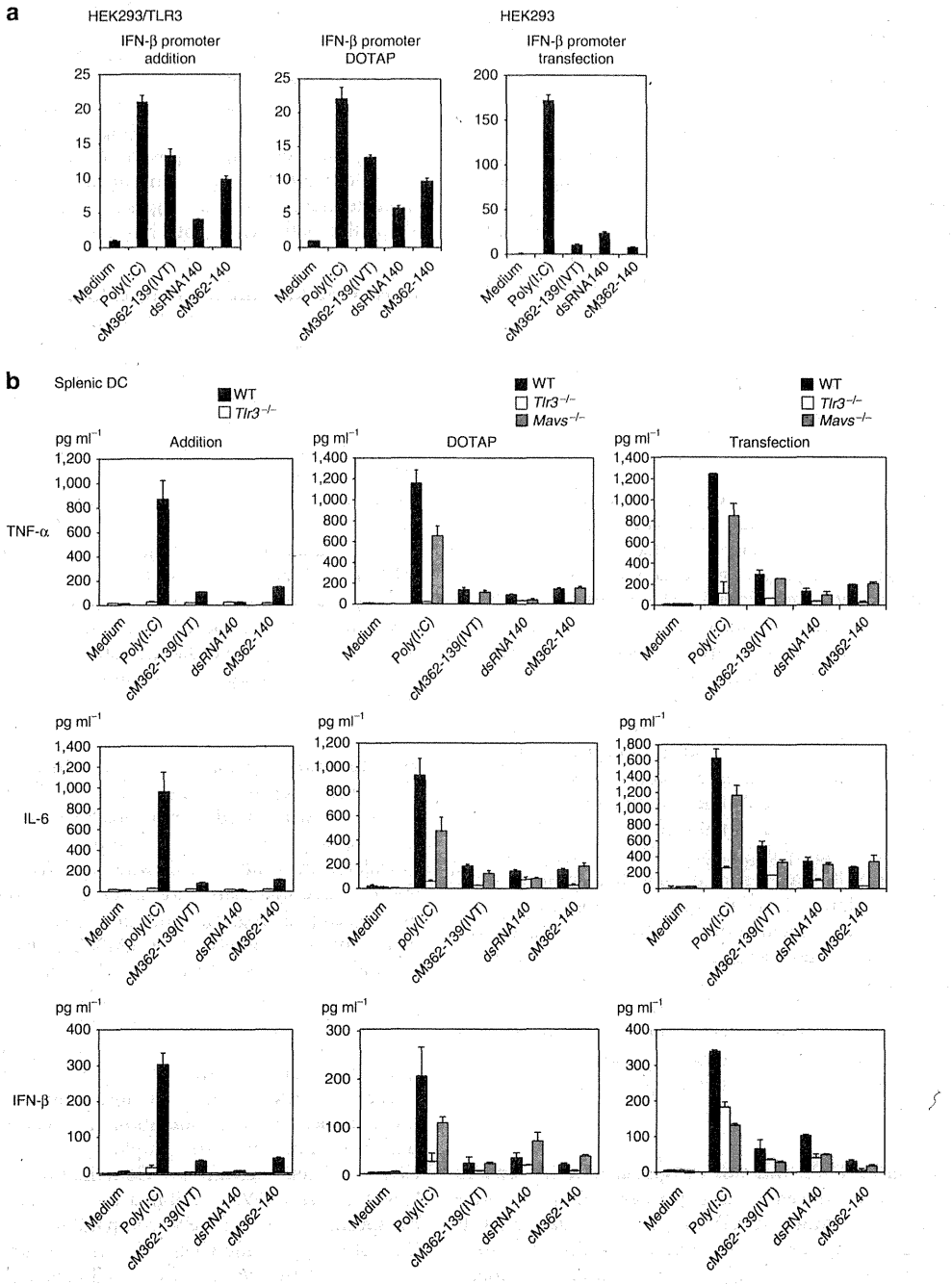

Figure 2 | TLR3-activating ability of cM362-140 in human and mouse cells. (**a**) TLR3-dependent IFN-β promoter activation by cM362-140. HEK293 cells were transiently transfected with IFN-β reporter and phRL-TK together with (left and middle panels) or without the expression plasmid for hTLR3 (right panel). Twenty-four hours after transfection, culture medium was removed and 10 μg ml^{-1} poly(I:C), cM362-139(IVT), dsRNA140 or cM362-140 in fresh medium (left panel), or the same compounds complexed with DOTAP liposomal reagent (middle panel), or with Lipofectamine 2000 (right panel) were added to cells. Luciferase activity was measured 6 h (left and middle panel) or 24 h (right panel) after stimulation, and expressed as fold induction relative to the activity of non-stimulated cells. Representative data from three independent experiments, each performed in triplicate, are shown (mean ± s.d.). (**b**) Splenic CD11c$^+$ DCs (1.0×10^6 per ml) isolated from *Tlr3*$^{-/-}$, *Mavs*$^{-/-}$ or WT mice were stimulated with 10 μg ml^{-1} untreated (left panels), DOTAP liposomal reagent-conjugated (middle panels) or Lipofectamine 2000-conjugated (right panel) nucleic acids as indicated. Twenty-four hours after stimulation, IFN-β in the culture supernatants was quantified using ELISA. TNF-α and IL-6 levels were measured using CBA. Representative data from three to five independent experiments are shown (mean ± s.d.).

treatment with cM362-140 caused barely any regression of EG7 tumours in this model (Fig. 5a). Nevertheless, combination therapy with OVA + cM362-140 still induced tumour growth retardation (Fig. 5a). OVA-specific CD8$^+$ T cells proliferated and activated in the mice stimulated with OVA + cM362-140, as assessed by tetramer assay (Fig. 5b) and IFN-γ production (Fig. 5c). We confirmed that the induction of OVA-specific CD8$^+$ T-cell activation by cM362-140 + OVA largely depends

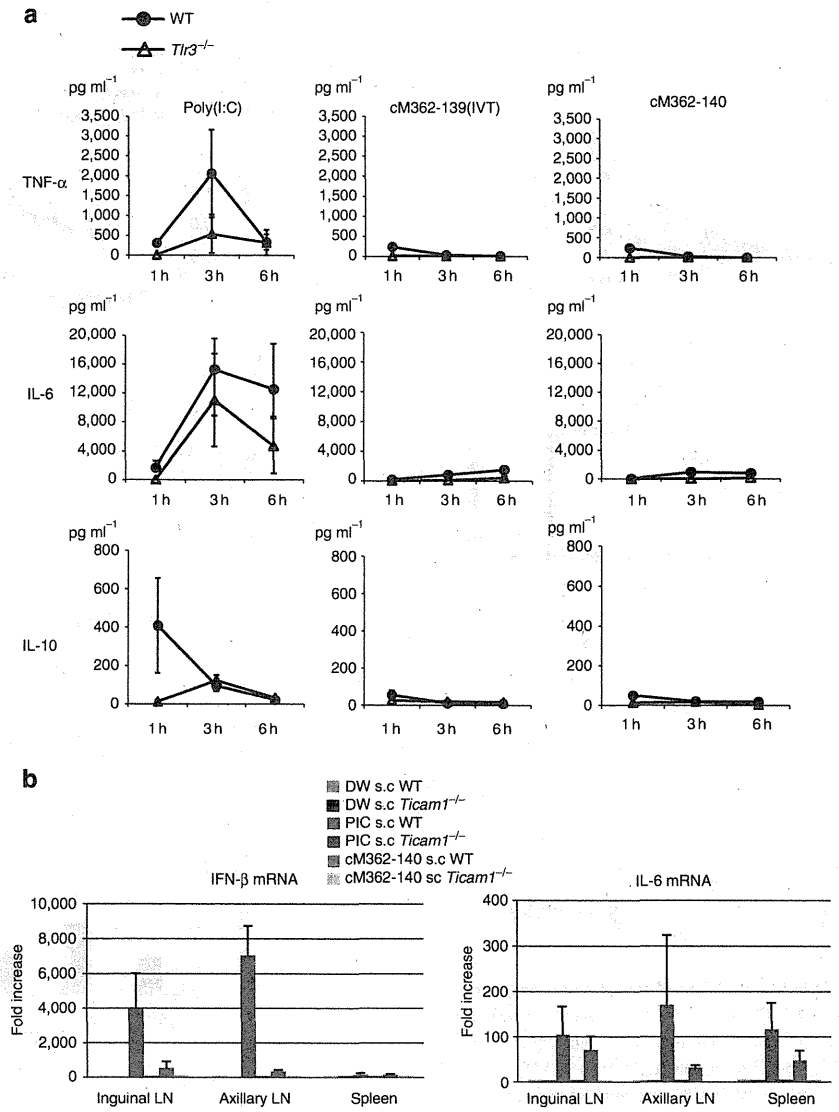

Figure 3 | cM362-139(IVT) and cM362-140 do not induce inflammatory cytokines. (**a**) Wild-type or *Tlr3*$^{-/-}$ female mice (9 week) were injected i.p. with 50 μg poly(I:C), cM362-139(IVT) or cM362-140 in RNase-free water. At timed intervals, blood was collected from the tail vein and TNF-α, IL-6 and IL-10 levels in each sample were measured using a CBA. Data are shown as the mean ± s.e.; $n=3$ mice per group. (**b**) Wild-type or *Ticam*$^{-/-}$ female mice were injected s.c. with distilled water (DW), poly(I:C) or cM362-140 in RNase-free water. After 6 h, spleen, inguinal and axillary LNs were harvested and *IFN-β* and *IL-6* mRNA expressions were quantified by qPCR. Data are expressed as the fold induction relative to the expression in DW-injected mice and shown as the mean ± s.e.; $n=3$ mice per group.

on TLR3/TICAM-1 using KO mice (Supplementary Fig. 9). Although polyI:C induces RIP1/3-mediated necroptosis via TICAM-1 in some tumour lines, cM362-140 was not the case in EG7 tumour (Supplementary Fig. 10). Hence, TLR3 has an important role in inducing cM362-140-mediated immune response and tumour growth retardation in the s.c. setting we employed in this study.

Antigen-specific CD8$^+$ T-cell priming by cM362-139/140. The Ag-specific CD8$^+$ T-cell priming ability of cM362-139/140 in tumour-free settings was next examined using spleen and inguinal LN cells. Wild-type mice were injected s.c. with OVA with or without RNA adjuvants twice per week. Since OVA-specific CD8$^+$ T cells most proliferated in spleen or inguinal LN 4 days after the last injection of OVA + poly(I:C) (Fig. 6a), spleen and LN cells were harvested from mice 4 days after the last adjuvant injection. cM362-139/140 significantly induced OVA-specific CD8$^+$ T-cell proliferation in the inguinal LN and spleen compared with poly(I:C) (Fig. 6b). OVA-specific IFN-γ production in spleen cells was also efficiently induced by cM362-139(IVT) and cM362-140 (Fig. 6c). The TICAM-1 pathway was mainly involved in Ag-specific CD8$^+$ T-cell activation induced by cM362-140 (Fig. 6d).

NK cell-mediated B16 tumour regression by cM362-139/140. Using a C57BL/6-B16 syngeneic NK-sensitive tumour-implant model[9], we evaluated NK-dependent antitumour activity of cM362-139(IVT) injected s.c. around the pre-formed tumour (Fig. 7a). Suppression of tumour growth, determined as reported previously[9], was observed in the group that received cM362-139(IVT) compared with the water-treated group. The retardation of B16 tumour growth appeared to depend on TLR3

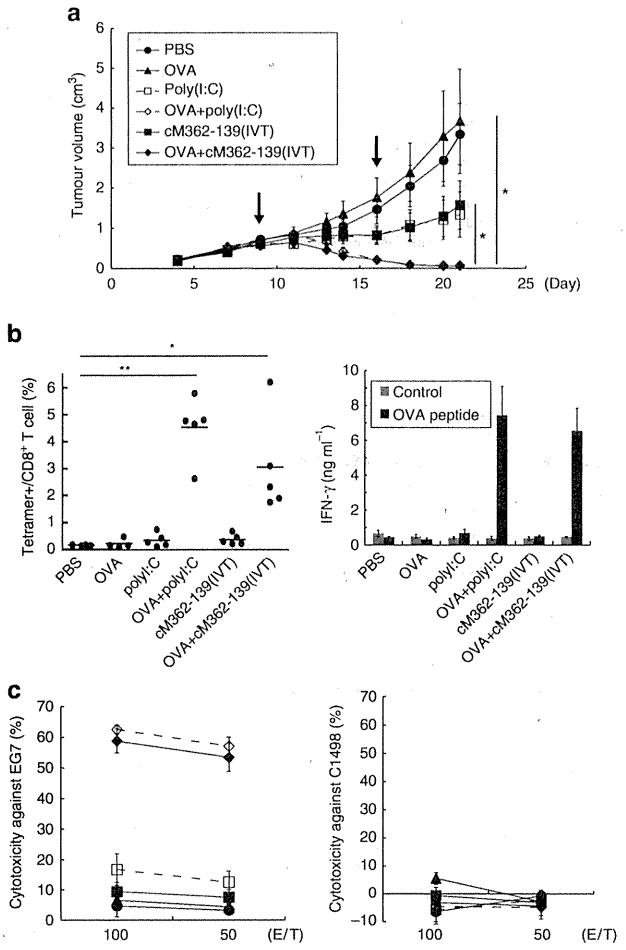

Figure 4 | cM362-139(IVT) induces CTL-mediated tumour regression. (**a**) Antitumour effect of cM362-139(IVT). WT mice were challenged with EG7 cells, and 7 and 14 days later they were s.c. injected with control PBS (●), OVA (▲), polyI:C (□) and OVA + polyI:C (◇) or cM362-139(IVT) (■) or OVA + cM362-139 (♦). Tumour size was evaluated in each group. All error bars used in this figure show ± s.e.m. Data are representative of two independent experiments. Each group consisted of five mice. $^{*}P<0.05$ (ANOVA with Bonferroni's test). (**b**) OVA-specific CTL induction by cM362-139(IVT). Left panel: spleen cells were harvested at day 21 (7 days after 2nd therapy) and the proportion of tetramer-positive cells/CD8$^+$ T cells was evaluated. $^{*}P<0.05$, $^{**}P<0.01$. Right panel: spleen cells were harvested at day 21 as for the left panel. The cells were stimulated with OVA peptide for 3 days and the level of IFN-γ in the culture supernatant was measured. (**c**) Ag-specific cytotoxicity induced by cM362-139(IVT). Splenocytes collected from tumour-bearing mice at day 21 were cultured in the presence of immorbilized EG7 for 5 days. Then, the cytotoxicity against EG7 (left panel) or C1498 (control, right panel) was measured by ^{51}Cr release assay.

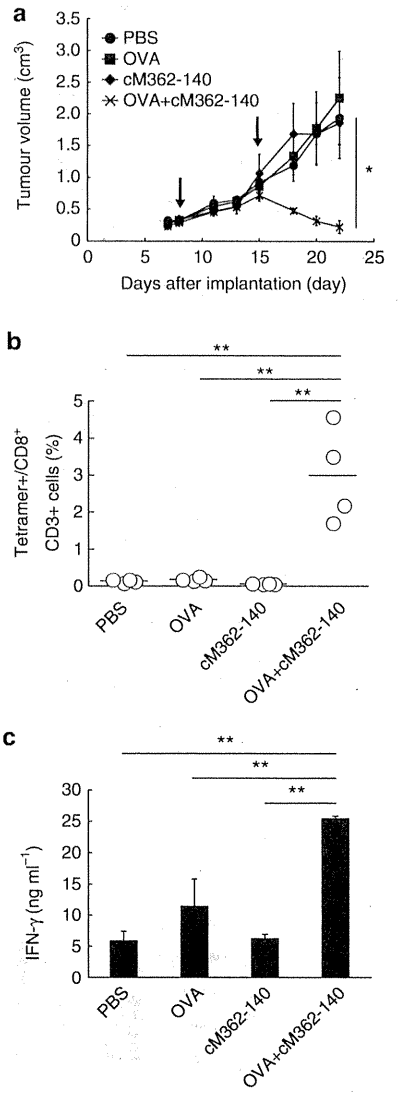

Figure 5 | cM362-140 induces EG7 tumour growth retardation. (**a**) Antitumour effect of cM362-140. As in Fig. 4, tumour-bearing mice were s.c. injected with PBS, OVA, cM362-140 and OVA + cM362-140 at timed intervals (days 8 and 15). Tumour size was evaluated in each group. (**b**) OVA-specific CTL induction by cM362-140. The proportion of tetramer-positive cells/CD8$^+$ T cells in spleen was evaluated at day 22 (7 days after 2nd therapy). (**c**) Ag-specific IFN-γ production induced by cM362-140. Splenocytes were harvested at day 22 and incubated with OVA peptides for 3 days. The level of IFN-γ in the supernatant was measured by ELISA. $^{*}P<0.05$, $^{**}P<0.01$ (ANOVA with Bonferroni's test).

and TICAM-1 (Fig. 7a,b). NK1.1$^+$ cells were involved in this tumour growth retardation (Fig. 7c), consistent with the NK-sensitive properties of B16 cells. No direct tumour cytolysis by macrophages[31] was associated with B16 growth retardation in the cM362-139(IVT) therapy. Splenocytes from the cM362-139(IVT)-treated group exerted higher cytotoxicity than those from the control group *in vitro* (Fig. 7d).

The chemically synthesized TLR3 ligand cM362-140 expressed a similar tumour-suppressing activity against B16 implant melanoma in the same model (Fig. 7e). This cM362-140-mediated NK-tumoricidal activity on B16 tumours was abrogated in *Ticam1*$^{-/-}$ mice (Fig. 7e). Thus, cM362-140 suppresses NK-sensitive tumours *in vivo* via TLR3 by acting as an NK-inducing adjuvant.

Discussion

Cancer immunotherapy relies on suitable adjuvants. Many TAA peptides have been synthesized, but the lack of an appropriate adjuvant to induce an immune response against the peptides has hampered progress in peptide vaccine therapy. Although many candidates, most of which were retrospectively recognized as TLR

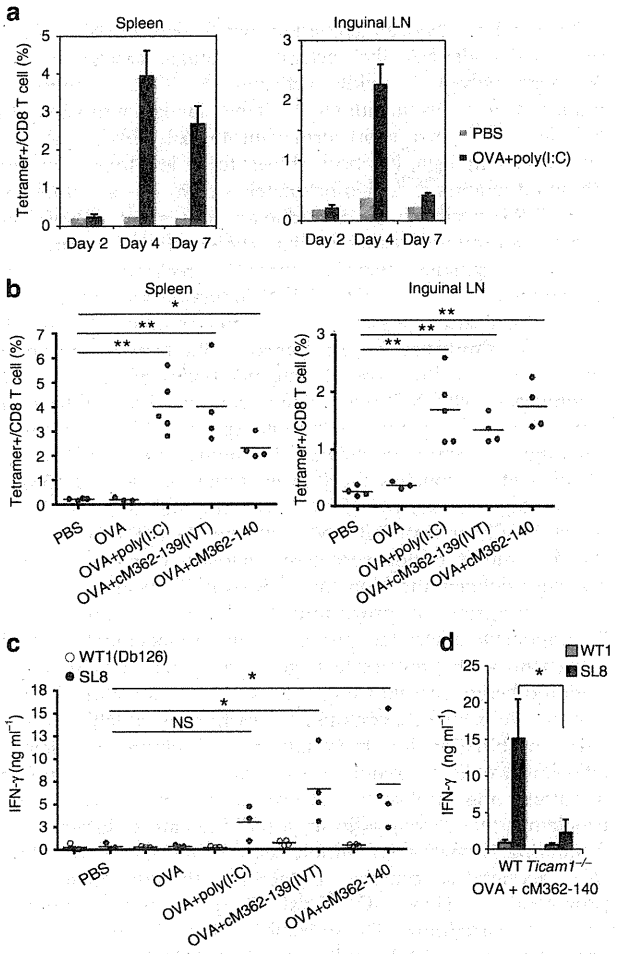

Figure 6 | cM362-139/140-induced antigen-specific CD8 T-cell activation in tumour-free settings. (**a**) Time-course experiments of poly(I:C)-induced antigen-specific CD8 T-cell activation in spleen and inguinal LN. WT mice were injected s.c. with 100 μl PBS or 50 μg poly(I:C) + 100 ng OVA twice per week. Spleen and inguinal LN cells were harvested at 2, 4 or 7 days after the last adjuvant injection and an increase of OVA-specific CD8 T-cell proliferation was evaluated with tetramer assay. (**b**,**c**) WT mice were injected s.c. with PBS, OVA, OVA + 50 μg poly(I:C), OVA + 50 μg cM362-139(IVT) or OVA + 70 μg cM362-140 twice per week. Spleen and inguinal LN cells were harvested 4 days after the last adjuvant injection and an increase of OVA-specific CD8 T-cell proliferation (**b**) and IFN-γ production (**c**) were then evaluated. (**b**) Proportion of tetramer-positive cells/CD8 T cells in spleen and inguinal LN. (**c**) Spleen cells were stimulated with OVA (SL8) or WT1 (Db126) peptide for 3 days and the level of IFN-γ in the culture supernatant was measured using a CBA. NS, no significant (>0.05), $^{*}P<0.05$, $^{**}P<0.01$, compared with PBS control (ANOVA with Dunnett's test). (**d**) cM362-140 + OVA induced Ag-specific CTL activation via the TICAM-1 pathway. Wild-type or *Ticam1*$^{-/-}$ mice were injected s.c. with PBS, OVA or OVA + cM362-140 as described above. Spleen cells were harvested 4 days after the last adjuvant injection and OVA-specific IFN-γ productions were assessed. PBS or OVA injection did not induce IFN-γ production from spleen cells. The data from OVA + cM362-140 injection are shown. $^{*}P<0.05$ (Student's *t*-test).

agonists, have been tested in humans[1,6], they have not yet been clinically approved because of their undesired effects.

In this study, we designed many nucleotide adjuvants and tested their functional properties. Our approach is timely since most dsRNA receptors have been identified in the mouse and

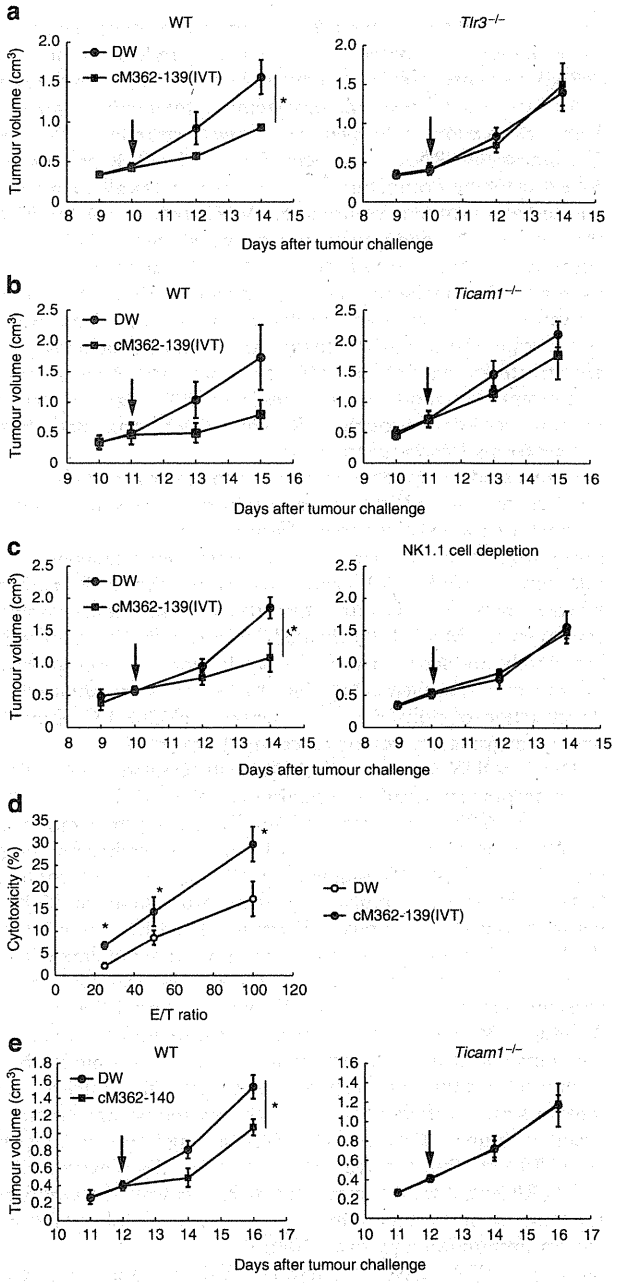

Figure 7 | Therapeutic effects of sODN-dsRNA in B16 tumour-implant model. (**a**,**b**) B16 tumour growth in mice after cM362-139(IVT) treatment. B16 melanoma cells were s.c. implanted into B6 WT mice (**a** and **b**), *Tlr3*$^{-/-}$ mice (**a**), or *Ticam1*$^{-/-}$ mice (**b**). cM362-139(IVT) or distilled water was injected s.c. around the tumour on the day indicated by arrow and then tumour volume was measured. Data are shown as tumour average volume ± s.e.; $n=3$ mice per group. $^{*}P<0.05$. (**c**) Effect of NK cell depletion on cM362-139(IVT) treatment. Tumour-bearing mice were injected with anti-NK1.1 antibody to deplete NK cells. After 24 h, cM362-139(IVT) or distilled water was injected into the mice as described in **a**. (**d**) Cytotoxic activity of DX5^{+} NK cells isolated from cM362-139(IVT)-treated mice. DX5^{+} cells were isolated from B16 tumour-bearing mice treated with cM362-139(IVT) or distilled water for 18 h. Cytotoxic activity of DX5^{+} cells against B16 target cells was measured by ^{51}Cr release assay. (**e**) B16 tumour growth in mice after cM362-140 treatment. Tumour-bearing mice were treated with cM362-140 as described in **a**.

human[1–4], and their structures and properties have been known for a decade[32–34]. Based on our current understanding of the dsRNA response, poly(I:C) activates both TICAM-1 (ref. 35) and MAVS pathways[36] resulting in systemic cytokinemia in mice[21,37]. Viral replication intermediates, double-stranded RNA and 5′-triphosphate RNA cause activation of the RLR pathway and robust cytokine production[38,39]. Here we chemically synthesized and tested a synthetic compound, cM362-140, an sODN-dsRNA that entered the endosomes and activated the TLR3/TICAM-1 pathway *in vivo*. Specifically, cM362-140 activated TLR3 in myeloid cells, including DCs in draining LNs, and induced activation of NK cells and proliferation of CTL. There was no systemically significant production of cytokines, including IFNs, after treatment with cM362-140. Our study establishes the proof-of-concept that modified or complexed RNA can regulate the immune response through TLR3 (refs 37,40), and that cM362-140 performs this function *in vivo*.

In this study, a systemic increase in the cytokine levels was not required for the induction of an antitumour immune response. Instead, a basal cytokine level effectively primed DCs to activate tumoricidal NK cells and CTL response. Subcutaneous or i.p. injection of cM362-140 barely activated the RLR pathway, whereas poly(I:C) activated this pathway to induce systemic cytokinemia. cM362-140 activated TICAM-1 for DC maturation, but barely induced chemokine production or necroptosis in tumour cells (Supplementary Fig. 10), which were reported as a direct action of poly(I:C)[29,30]. Therefore, cM362-140 eliminates major inflammatory responses caused by poly(I:C).

The 5′-sODN sequence of cM362-140 targeted the dsRNA to the endosome and evaded recognition by RIG-I/MDA5. A 140-bp stretch of dsRNA was required for TLR3 multimerization and TICAM-1 activation, but unsatisfactory for endosome targeting[40,41]. The 5′-sODN sequence of cM362 does not contain a CpG motif, which stimulates cytokine production via TLR9 in plasmacytoid DC. To prevent Dicer-mediated RNA interference, RNA sequences specific to human mRNAs were not employed. In addition, the antisense 5′-end of cM362-140 was OH, neither phosphorylated nor capped, unlike viral or host RNA products. Although cM362-140 was an artificial compound to circumvent host innate sensors, its constituents are native and modifiable to maximize antitumour response. Although the nucleic acid-sensing system differs somewhat between mouse and human[2,4]: generally, human BDCA3$^+$ DCs express a high level of TLR3 but no TLR9 (ref. 20), whereas mouse CD8α^+ DCs express TLR3 and TLR9 (refs 2,18,41), extrapolating results from the mouse and applying them to the human will be crucial for establishing human immunotherapy in the future.

Type I IFNs have remarkable antiviral and antitumour properties, but sometimes elicit severe side effects during treatment in patients. For example, s.c. injection of poly(I:C) induces inflammation, erythema and fever[42]. In clinical trials, cancer patients cannot tolerate high doses of poly(I:C), even if administered via s.c. injection[11,42–44]. Poly(I:C) consists of polyI and polyC chains of variable lengths that differ in function from one batch to the next, and, for unknown reasons, exogenous poly(I:C) activates cytoplasmic RNA sensors[36]. By contrast, cM362-140 is uniform. It binds TLR3 and fails to activate cytoplasmic RNA sensors, indicating that immune modulation by RNA occurs only in the draining LNs and tumour microenvironment[45]. Thus, cM362-140 enables us with a 'defined' immunotherapy to patients without systemic cytokine response or inflammation.

Several compounds that activate the TICAM-1 pathway are clinically available. Monophosphoryl lipid A is a TLR4 adjuvant that activates the TICAM-2/TICAM-1 cascade via TLR4/MD-2 (ref. 46). However, monophosphoryl lipid A still retains the TLR4-mediated MyD88 activation, which conceptually different from sODN-dsRNA that activates a single cascade of PRR. Although poly(A:U) mildly activates the TLR3 pathway and induces type I IFN in humans[47], it has far less adjuvancy than poly(I:C)[6,28,48]. In a short-term clinical trial, poly(I:C$_{12}$U), also known as ampligen, has been shown to be less toxic than other immunotherapies[49,50]. Unfortunately, data on its uniformity and TLR3-specificity as an adjuvant are scant. Poly(I:C)LC, another antitumour adjuvant, has shown clinical promise, but it causes cytokine toxicity, thereby precluding its further development[5,6,42–44,51]. Type I IFN induction and the output of IFNAR activation appear to be predominant in low-dose poly(I:C) administration in human volunteers[42]. In another clinical study, a low dose (1.4 mg per body) of poly(I:C)LC in combination with NY-Eso-1, which contains TAA epitopes, has been shown to mount a tumour-specific T-cell response[11]. Although low doses of poly(I:C)LC induce type I IFN, it only insufficiently stimulates T-cell proliferation *in vivo*[11]. cM362-140 is advantageous over poly(I:C)LC in that a high dose can be used to specifically activate TICAM-1, but not MAVS *in vivo*. This is the first report of the successful chemical creation of a long, sequence-defined and bioactive TLR3-specific ligand.

The targeting of programmed cell death-1 and cytotoxic T-lymphocyte-associated protein-4 with monoclonal antibodies in patients with progressive-staged cancer may provide another immunotherapy breakthrough[52]. Except for an alum adjuvant that can induce a Th2 response[2,53], there is no suitable adjuvant-TAA combination for immunotherapy. Immune enhancing by adjuvant would be required since tumour cells can undergo mutations and survive to circumvent immune attack. A main problem is that current adjuvant candidates are all inflammatory, facilitating formation of tumour-supporting microenvironment, that accelerates genome instability, tumour growth and progression[45]. Here, sODN-dsRNA is a non-inflammatory adjuvant sustaining DC-mediated NK/CTL activation, its combining with TAAs will bring a therapeutic benefit to a number of patients with intractable tumours.

Methods

Cell culture, reagents and plasmid. HEK293 cells were maintained in Dulbecco's Modified Eagle's medium (Invitrogen) supplemented with 10% heat-inactivated FCS (Invitrogen) and antibiotics. HeLa cells were kindly provided by Dr T. Fujita (Kyoto University) and maintained in Eagle's minimal essential medium (Nissui,) supplemented with 1% L-glutamine and 5% FCS. B16D8 melanoma cells were cultured at 37 °C under 5% CO_2 in RPMI containing 10% FCS, penicillin and streptomycin. EG7 and C1498 cells were purchased from ATCC and cultured in RPMI-1640 supplemented with 10% FCS, 55 μM 2-mercaptoethanol (2-ME) and 1 mM sodium pyruvate, and RPMI-1640 supplemented with 10% FCS and 25 ng ml^{-1} 2-ME, respectively. Poly(I:C) was purchased from Amersham Biosciences. Endotoxin-free ovalbumin was purchased from Hyglos. $OVA_{257-264}$ peptide (SL8), control WT1 peptide (Db126) and OVA ($H2K^b$-SL8) tetramer were from MBL. Human serum type AB was from Lonza. ODNs were synthesized by GeneDesign. Following antibodies were used in this study: Alexa Fluor-568-conjugated secondary antibody (Invitrogen), FITC-CD8α (53-6.7) and APC-CD3ε (145-2C11) (BioLegend), and PerCP/Cy5.5-7AAD (BD Biosciences). The human TLR3 expression plasmid was constructed in our laboratory[33].

Preparation of *in vitro* transcribed sODN-dsRNAs. The leader-trailer sequence of a MV laboratory-adapted strain of Edmonston was used as the dsRNA template[25]. DNA fragments covering this region of the MV genome and the T7 promoter sequence were amplified using PCR with specific primers and the plasmid pCR-T7 MV as a template. Sense and antisense MV RNAs from the PCR products were *in vitro* transcribed using an AmpliScribe T7 transcription kit (Epicentre Technologies) according to the manufacturer's protocol. The transcribed products were purified by 8% PAGE containing 7 M urea. After visualization by ultraviolet illumination, the appropriate bands were excised and eluted with 0.3 M sodium acetate. The eluted RNAs were ethanol precipitated and resuspended in RNase-free water. For large-scale preparation of RNAs, electro-elutions were performed using D-Tube Dialyzer Maxi (Novagen) and eluted RNAs were dialyzed, concentrated and precipitated with ethanol. The concentration of RNA was determined by measuring the absorbance at 260 nm in a

spectrophotometer. To generate sODN-dsRNA, sODN + linker DNA, sense and antisense RNA were mixed and annealed. sODNs, MV RNA sequences in sODN-dsRNA and PCR primers used in this study are described in Supplementary Tables 1–3.

Preparation of cM362-140. The chemically synthesized long RNAs as an alternative to *in vitro* transcribed RNAs were completed by a ligation reaction mediated by splint DNA[54] with slight modification. The outline of chemical synthesis was described below.

To prepare the sense strand of cM362-140, the ligation reactions were performed in two steps. First, S2 RNA (40 nmol), S3 RNA (40 nmol) and specific splint DNA (40–48 nmol) were mixed, heated at 90 °C for 5 min and slowly cooled to 4 °C (Supplementary Table 4A,B). Following hybridization, T4 DNA ligase (Takara) was added and incubated at room temperature for 16–22 h. The ligation reaction mixtures comprised 15.4 μM annealed complex, 66 mM Tris-HCl (pH 7.6), 6.6 mM $MgCl_2$, 10 mM DTT, 0.1 mM ATP and ~31 U μl^{-1} T4 DNA ligase. As the second ligation, S1 cM362-RNA (40 nmol) and the specific splint DNA (40–48 nmol) for the second ligation site were added into the first ligation reaction mixture, hybridized and T4 DNA ligase was added. The mixture was incubated at room temperature for 16–22 h. The derived full-length 165 mer sense strand was isolated by 8% PAGE containing 7 M urea and electro-elution. The subsequent procedure was the same as described in the section describing purification of *in vitro* transcribed RNAs. Overall yield was 8–10%.

To prepare the antisense RNA of cM362-140, three fragment RNAs, AS1, AS2 and AS3 (33 nmol each) and the related splint DNAs (33 nmol each) were mixed, hybridized and then T4 DNA ligase was added. The mixture was incubated at room temperature for 16–22 h. The following procedure was the same as described above. Overall yield was 15–22%. To generate cM362-140, sense- and antisense-RNAs were annealed.

Analysis with microchip electrophoresis. To analyse the cM362-139 complex, we used a microchip electrophoresis instrument (model SV1210; Hitachi Electronics Engineering Co. Ltd.). The standard procedure for electrophoresis using 2-mercaptoethanol (ME) has been previously described[55,56]. sODN or RNAs were adjusted to 0.2 μM with water. The sODN/RNA1/RNA2 complex (designated cM362-139) and dsRNA (RNA1 + RNA2) were prepared by mixing DNA or RNAs and hybridizing in water (final concentration 0.4 μM). The sample solution (10 μl) was applied to the sample well of the microchip device and the programme was run at 600 V for 120 s (injection time), then at 1,100 V for 180 s (separation time) under 350 V of return voltage at 20 °C. During the electric separation, DNA or RNA peaks were detected by laser induced fluorescence and analysed.

Agarose gel electrophoresis. cM362-139(IVT) and cM362-140 were incubated in PBS or in RNase-free water with or without serum, for 60 min at 37 °C or 42 °C. Aliquots containing 0.1–0.2 μg of incubated sODN-dsRNAs were then mixed with 10 × loading dye (Takara Bio Inc.) and loaded onto 3 or 4% agarose gel (Nusieve 3:1 Agarose, Lonza) containing ethidium bromide. After electric separation, nucleic complexes were visualized using ultraviolet transilluminator (FAS-III, Toyobo).

Reporter gene assay. HEK293 cells (8×10^5 cells per well) were cultured in six-well plates and transfected with the TLR3 expression vector or empty vector (400 ng per well) together with the reporter plasmid (400 ng per well) and an internal control vector, phRL-TK (Promega; 20 ng per well) using Lipofectamine 2000 (Invitrogen). The p-125 luc reporter containing the human IFN-β promoter region (−125 to +19) was provided by Dr T. Taniguchi (University of Tokyo). Twenty-four hours after transfection, cells were collected and resusupended in medium with or without FCS. Then, cells were seeded into 96-well plates and stimulated with the indicated RNAs for 6 h. The *Firefly* and *Renilla* luciferase activities were determined using a dual-luciferase reporter assay kit (Promega). The *Firefly* luciferase activity was normalized to the *Renilla* luciferase activity and was expressed as the fold induction relative to the activity in unstimulated vector-transfected cells. All assays were performed in triplicate.

Cytokine assay. Splenic $CD11c^+$ DCs from wild-type, $Tlr3^{-/-}$ or $Mavs^{-/-}$ mice were prepared as described previously[9,31]. Cells were suspended in RPMI-1640 (Invitrogen) supplemented with 10% heat-inactivated FCS and antibiotics and stimulated with the indicated RNAs. Twenty-four hours after stimulation, culture supernatants were collected and analysed for cytokine levels by ELISA or Cytometric Bead Array (CBA). ELISA kits for mouse IFN-α and IFN-β were purchased from PBL Biomedical Laboratories. CBA *flex sets* for mouse IL-6 and TNF-α were purchased from BD Bioscience. Experiments were performed according to the manufacturer's instructions and samples were analysed using the Facs Aria (BD Bioscience).

Confocal microscopy. HeLa cells (1.0×10^5 cells per well) were cultured on microcover glasses (Matsunami Glass Ind., Ltd) in a 12-well plate. Three hours after seeding, cells were transfected with GFP-fused Rab5a or Lamp1 using BacMam systems (Cell Light Early Endosomes-GFP BacMam 2.0 or Cell Light Lysosomes-GFP BacMam 2.0, Life technologies) or left untreated. Sixteen hours after transfection, cells were incubated with 15 μg ml^{-1} Cy3-labelled cM362, cM362-dsRNAs or dsRNAs for 30 min at 4 °C. Cells were washed twice and further incubated at 37 °C. And then, cells were fixed with 4% paraformaldehyde at the time points indicated. The coverslips were mounted onto slide glass with Prolong Gold with DAPI for nuclei staining. Cells were visualized at a × 63 magnification using a Zeiss LSM520 META microscope (Carl Zeiss Microscopy GmbH).

Quantitative PCR (qPCR). Total RNA was extracted using the Trizol reagent (Qiagen) and reverse-transcribed using a high-capacity cDNA Reverse Transcripition kit (Applied Biosystems) and random primers according to the manufacturer's instructions. QPCR was performed using specific primers for mouse *GAPDH*, *IFN-β*, *IL-6* and *TNF-α* (Supplementary Table 5) and the Step One Real-time PCR system (Applied Biosystems).

Mice. $Ticam1^{-/-}$ and $Mavs^{-/-}$ mice were made in our laboratory and back-crossed more than eight times to adapt C57BL/6 background[9,10]. Inbred C57BL/6 WT mice were purchased from CLEA Japan. $Tlr3^{-/-}$ mice were kindly provided by Dr S. Akira (Osaka University). Mice were maintained under specific pathogen-free conditions in the animal facility of the Hokkaido University Graduate School of Medicine. Female mice 6–12 weeks of age were used in all experiments, all of which were performed according to the guidelines issued by the Hokkaido University Animal Care and Use Committee.

***In vivo* mouse cytokine assay.** Wild-type and $Tlr3^{-/-}$ mice (9 weeks) were injected i.p. with 50 μl (50 μg) poly(I:C), cM362-139 (IVT) or cM362-140, and blood was collected from the tail vein at timed intervals. Cytokine levels in sera were measured using a CBA. In some cases, wild-type and $Ticam1^{-/-}$ mice were s.c. injected with 75 μl (75 μg) poly(I:C) or cM362-140. After 6 h, mice were killed and draining inguinal LN, axillary LN and spleen were harvested[10]. *IFN-β*, *IL-6* or *TNF-α* mRNA expression in these lymphoid organs was measured by qPCR.

Tumour challenge and sODN-dsRNA treatment. Mice 6–10 weeks of age were used in all experiments. Mice were shaved at the back and injected s.c. with 200 μl of 6×10^5 B16D8 cells in PBS (−). Tumour volumes were measured at regular intervals using a caliper[9]. Tumour volume was calculated using the following formula: tumour volume (cm^3) = (long diameter) × (short diameter)^2 × 0.4. 75 μl (75 μg) sODN-dsRNAs or distilled water with no detectable LPS was mixed with *in vivo*-JetPEI (Polyplus), a polymer-based transfection reagent, according to the manual and then injected s.c. around the tumour. Treatment was started when the average tumour volume of 0.4–0.6 cm^3 was reached. To deplete NK cells, we injected titrated anti-NK1.1 ascites (PK136) i.p. in tumour-bearing mice the day before sODN-dsRNA treatment. Depletion of $NK1.1^+$ cells was verified by flow cytometory.

In the case of EG7 cell challenge, mice were injected s.c. with 200 μl of 2×10^6 syngenic EG7 cells in PBS (−). When the average tumour volumes reached ~0.6 cm^3, 50 μl of 100 μg endotoxin-free ovalbumin in PBS (−) with or without 50 μl of 50 μg poly(I:C) or sODN-dsRNA was injected s.c. around the tumour. PBS (−) (100 μl) was used as a control. Treatments were performed twice per week.

CTL activity in tumour-bearing mice after adjuvant therapy. Female mice 6–10 weeks of age were used for this study. Splenocytes were harvested from tumour-bearing mice at 7 days after the last adjuvant treatment. In the case of tumour-free settings, spleen and inguinal LN cells were harvested from wild-type or $Ticam1^{-/-}$ mice 4 days after the last adjuvant injection. The cells were stained with FITC-CD8α (1:200), PerCP/Cy5.5-7AAD (1:200), APC-CD3ε (1:200) and PE-OVA-tetramer (1:50) to detect Ag-specific $CD8^+$ T cells. To evaluate cytokine production, splenocytes (2×10^6 per 200 μl per well) were cultured for 3 days in the presence of 100 nM OVA peptide (SL8: SIINFEKL) or control WT1 peptide (Db126: RMFPNAPYL) and IFN-γ production was analysed with CBA or ELISA. To assess the cytotoxic activity of CTLs, splenocytes (1×10^6 per ml) were co-cultured with mitomycin C-treated EG7 cells (5×10^5 per ml) in the presence of 10 U ml^{-1} IL-2 for 5 days. Then, the cells were incubated with ^{51}Cr-labelled EG7 or C1498 cells for 4 h and determined cytotoxic activity[10]. The cytotoxicity was calculated by this formula: Cytotoxicity (%) = [(experimental release − spontaneous release)/(total release—spontaneous release)] × 100.

Cytotoxic activity assay of NK cells. Mice bearing B16 tumour were injected s.c. with cM362-139(IVT) mixed with *in vivo*-JetPEI. After 18 h, mice were killed and $DX5^+$ NK cells were isolated from spleen using DX5-positive selection microbeads (Miltenyi) according to the manual[9]. B16 cells were labelled with ^{51}Cr for 1 h and then washed three times with medium. $DX5^+$ cells and ^{51}Cr-labelled B16 cells were co-cultured at the indicated ratio[31]. After 4 h, supernatants were harvested and ^{51}Cr release was measured in each sample. Specific lysis was calculated by the following formula: cytotoxicity (%) = [(experimental release − spontaneous release)/(total release − spontaneous release)] × 100.

Statistical analysis. The significance of differences between groups was determined by the Student's *t*-test. In tumour-implant or -free mouse experiments, one-way analysis of variance with Bonferroni's multiple-comparison test or Dunnett's test was performed to analyse statistical significance.

References

1. Akira, S., Uematsu, S. & Takeuchi, O. Pathogen recognition and innate immunity. *Cell* **124,** 783–801 (2006).
2. Gürtler, C. & Bowie, A. G. Innate immune detection of microbial nucleic acids. *Trends Microbiol.* **21,** 413–420 (2013).
3. Seya, T. *et al.* Role of Toll-like receptors and their adaptors in adjuvant immunotherapy for cancer. *Anticancer Res.* **23,** 4369–4376 (2003).
4. Matsumoto, M. & Seya, T. TLR3: interferon induction by double-stranded RNA including poly(I:C). *Adv. Drug Deliv. Rev.* **60,** 805–812 (2008).
5. Levine, A. S. & Levy, H. B. Phase I-II trials of poly IC stabilized with poly-L-lysine. *Cancer Treat. Rep.* **62,** 1907–1912 (1978).
6. Galluzzi, L. *et al.* Trial watch: experimental Toll-like receptor agonists for cancer therapy. *OncoImmunology* **1,** 699–716 (2012).
7. Lvovsky, E. A., Mossman, K. L., Levy, H. B. & Dritschilo, A. Response of mouse tumor to interferon inducer and radiation. *Int. J. Radiat. Oncol. Biol. Phys.* **11,** 1721–1725 (1985).
8. Talmadge, J. E. *et al.* Immunotherapeutic potential in murine tumor models of polyinosinic-polycytidylic acid and poly-L-lysine solubilized by carboxymethyl cellulose. *Cancer Res.* **45,** 1066–1072 (1985).
9. Akazawa, T. *et al.* Antitumor NK activation induced by the Toll-like receptor 3-TICAM-1 (TRIF) pathway in myeloid dendritic cells. *Proc. Natl Acad. Sci. USA* **104,** 252–257 (2007).
10. Azuma, M., Ebihara, T., Oshiumi, H., Matsumoto, M. & Seya., T. Cross-priming for antitumor CTL induced by soluble Ag + poly I:C depends on the TICAM-1 pathway in mouse CD11c(+)/CD8α(+) dendritic cells. *Oncoimmunology* **1,** 581–592 (2012).
11. Sabbatini, P. *et al.* Phase I trial of overlapping long peptides from a tumor self-antigen and poly-ICLC shows rapid induction of integrated immune response in ovarian cancer patients. *Clin. Cancer Res.* **18,** 6497–6508 (2012).
12. Yoneyama, M., Onomoto, K. & Fujita, T. Cytoplasmic recognition of RNA. *Adv. Drug Deliv. Rev.* **60,** 841–846 (2008).
13. Dixit, E. & Kagan, J. C. Intracellular pathogen detection by RIG-I-like receptors. *Adv. Immunol.* **117,** 99–125 (2013).
14. Matsumoto, M. *et al.* Subcellular localization of Toll-like receptor 3 in human dendritic cells. *J. Immunol.* **171,** 3154–3162 (2003).
15. Sun, J. C., Beilke, J. N. & Lanier, L. L. Adaptive immune features of natural killer cells. *Nature* **457,** 557–561 (2009).
16. Fernandez, N. C. *et al.* Dendritic cells directly trigger NK cell functions: cross-talk relevant in innate anti-tumor immune responses in vivo. *Nature Med.* **5,** 405–411 (1999).
17. Schulz, O. *et al.* Toll-like receptor 3 promotes cross-priming to virus-infected cells. *Nature* **433,** 887–892 (2005).
18. Villadangos, J. A. & Shortman, K. Found in translation: the human equivalent of mouse CD8 + dendritic cells. *J. Exp. Med.* **207,** 1131–1134 (2010).
19. Edelson, B. T. *et al.* Peripheral CD103 + dendritic cells form a unified subset developmentally related to CD8alpha + conventional dendritic cells. *J. Exp. Med.* **207,** 823–836 (2010).
20. Jongbloed, S. L. *et al.* Human CD141 + (BDCA-3) + dendritic cells (DCs) represent a unique myeloid DC subset that cross-presents necrotic cell antigens. *J. Exp. Med.* **207,** 1247–1260 (2010).
21. Kato, H. *et al.* Differential roles of MDA5 and RIG-I helicases in the recognition of RNA viruses. *Nature* **441,** 101–105 (2006).
22. Okahira, S. *et al.* Interferon-beta induction through Toll-like receptor 3 depends on double-stranded RNA structure. *DNA Cell Biol.* **24,** 614–623 (2005).
23. Itoh, K., Watanabe, A., Funami, K., Seya, T. & Matsumoto, M. The clathrin-mediated endocytic pathway participates in dsRNA-induced IFN-beta production. *J. Immunol.* **181,** 5522–5529 (2008).
24. Liu, L. *et al.* Structural basis of Toll-like receptor 3 signaling with double-stranded RNA. *Science* **320,** 379–381 (2008).
25. Shingai, M. *et al.* Differential type I IFN-inducing abilities of wild-type versus vaccine strains of measles virus. *J. Immunol.* **179,** 6123–6133 (2007).
26. Miyake, T. *et al.* Poly I:C-induced activation of NK cells by CD8 alpha + dendritic cells via the IPS-1 and TRIF-dependent pathways. *J. Immunol.* **183,** 2522–2528 (2009).
27. Zhang, Z. *et al.* DDX1, DDX21, and DHX36 helicases form a complex with the adaptor molecule TRIF to sense dsRNA in dendritic cells. *Immunity* **34,** 866–878 (2011).
28. Gauzzi, M. C., Del Cornò, M. & Gessani, S. Dissecting TLR3 signalling in dendritic cells. *Immunobiology* **215,** 713–723 (2010).
29. Conforti, R. *et al.* Opposing effects of Toll-like receptor (TLR3) signaling in tumors can be therapeutically uncoupled to optimize the anticancer efficacy of TLR3 ligands. *Cancer Res.* **70,** 490–500 (2010).
30. Paone, A. *et al.* Toll-like receptor 3 triggers apoptosis of human prostate cancer cells through a PKC-alpha-dependent mechanism. *Carcinogenesis* **29,** 1334–1342 (2008).
31. Ebihara, T. *et al.* Identification of a polyI:C-inducible membrane protein that participates in dendritic cell-mediated natural killer cell activation. *J. Exp. Med.* **207,** 2675–2687 (2010).
32. Alexopoulou, L., Holt, A. C., Medzhitov, R. & Flavell, R. A. Recognition of double stranded RNA and activation of NF-kappaB by Toll-like receptor 3. *Nature* **413,** 732–738 (2001).
33. Matsumoto, M., Kikkawa, S., Kohase, M., Miyake, K. & Seya, T. Establishment of a monoclonal antibody against human Toll-like receptor 3 that blocks double-stranded RNA-mediated signaling. *Biochem. Biophys. Res. Commun.* **293,** 1364–1369 (2002).
34. Shime, H. *et al.* Toll-like receptor 3 signaling converts tumor-supporting myeloid cells to tumoricidal effectors. *Proc. Natl. Acad. Sci. U. S. A.* **109,** 2066–2071 (2012).
35. Oshiumi, H., Matsumoto, M., Funami, K., Akazawa, T. & Seya, T. TICAM-1, an adaptor molecule that participates in Toll-like receptor 3-mediated interferon-beta induction. *Nat. Immunol.* **4,** 161–167 (2003).
36. Yoneyama, M. *et al.* The RNA helicase RIG-I has an essential function in double-stranded RNA-induced innate antiviral responses. *Nat. Immunol.* **5,** 730–737 (2004).
37. Seya, T., Azuma, M. & Matsumoto, M. Targeting TLR3 with no RIG-I/MDA5 activation is effective in immunotherapy for cancer. *Expert Opin. Ther. Targets.* **17,** 533–544 (2013).
38. Hornung, V. *et al.* RNA is the ligand for RIG-I. *Science* **314,** 994–997 (2006).
39. Pichlmair, A. *et al.* RIG-I-mediated antiviral responses to single-stranded RNA bearing 5′-phosphates. *Science* **314,** 997–1001 (2006).
40. Tatematsu, M., Nishikawa, F., Seya, T. & Matsumoto, M. Toll-like receptor 3 recognizes incomplete stem structures in single-stranded viral RNA. *Nat. Commun.* **4,** 1833 (2013).
41. Jelinek, I. *et al.* TLR3-specific double-stranded RNA oligonucleotide adjuvants induce dendritic cell cross-presentation, CTL responses, and antiviral protection. *J. Immunol.* **186,** 2422–2429 (2011).
42. Caskey, M. *et al.* Synthetic double-stranded RNA induces innate immune responses similar to a live viral vaccine in humans. *J. Exp. Med.* **208,** 2357–2366 (2011).
43. Levy, H. B., Low, L. W. & Rabson, A. S. Inhibition of tumor growth by polyinosinic-polycytidylic acid. *Proc. Natl Acad. Sci. USA* **62,** 357–361 (1969).
44. Levine, A. S., Sivulich, M., Wiernik, P. H. & Levy, H. B. Initial clinical trials in cancer patients of polyriboinosinic-polyribocytidylic acid stabilized with poly-L-lysine, in carboxymethylcellulose [poly(ICLC)], a highly effective interferon inducer. *Cancer Res.* **39,** 1645–1650 (1979).
45. Lin, W. W. & Karin, M. A cytokine-mediated link between innate immunity, inflammation, and cancer. *J. Clin. Invest.* **117,** 1175–1183 (2007).
46. Mata-Haro, V. *et al.* The vaccine adjuvant monophosphoryl lipid A as a TRIF-biased agonist of TLR4. *Science* **316,** 1628–1632 (2007).
47. Sugiyama, T. *et al.* Immunoadjuvant effects of polyadenylic:polyuridylic acids through TLR3 and TLR7. *Int. Immunol.* **20,** 1–9 (2008).
48. Perrot, I. *et al.* TLR3 and Rig-like receptor on myeloid dendritic cells and Rig-like receptor on human NK cells are both mandatory for production of IFN-gamma in response to double-stranded RNA. *J. Immunol.* **185,** 2080–2088 (2010).
49. Gowen, B. B. *et al.* TLR3 is essential for the induction of protective immunity against Punta Toro Virus infection by the double-stranded RNA (dsRNA), poly(I:C12U), but not Poly(I:C): differential recognition of synthetic dsRNA molecules. *J. Immunol.* **178,** 5200–5208 (2007).
50. Jasani, B., Navabi, H. & Adams, M. Ampligen: a potential toll-like 3 receptor adjuvant for immunotherapy of cancer. *Vaccine* **27,** 3401–3404 (2009).
51. Hafner, A. M., Corthésy, B. & Merkle, H. P. Particulate formulations for the delivery of poly(I:C) as vaccine adjuvant. *Adv. Drug Deliv. Rev.* **65,** 1386–1399 (2013).
52. Intlekofer, A. M. & Thompson, C. B. At the bench: preclinical rationale for CTLA-4 and PD-1 blockade as cancer immunotherapy. *J. Leukoc. Biol.* **94,** 25–39 (2013).
53. Desmet, C. J. & Ishii, K. J. Nucleic acid sensing at the interface between innate and adaptive immunity in vaccination. *Nat. Rev. Immunol.* **12,** 479–491 (2012).
54. Jing, X. u., Lapham, J. & Crothers, D. M. Determining RNA solution structure by segmental isotopic labeling and NMR: Application to *Caenorhabditis elegans* spliced leader RNA 1. *Proc. Natl Acad. Sci. USA* **93,** 44–48 (1996).
55. Nishikawa, F., Arakawa, H. & Nishikawa, S. Application of microchip electrophoresis in the analysis of RNA aptamer-protein interactions. *Nucleos. Nucleot. Nucl. Acids* **25,** 369–382 (2006).
56. Nishikawa, F., Murakami, K., Matsugami, A., Katahira, M. & Nishikawa, S. Structural studies of an RNA aptamer containing GGA repeats under ionic conditions using microchip electrophoresis, circular dichroism, and 1D-NMR. *Oligonucleotides* **19,** 179–190 (2009).

Acknowledgements

We are grateful to Dr H. Nankai (GeneDesign, Inc., Osaka) for helping chemical synthesis of RNA. Technical and clerical assistance by Dr R. Hatsugai, and Ms H. Sato in our laboratory is gratefully acknowledged. We appreciate Dr K. Toyoshima (RIKEN, Tokyo) for organizing the start of this project.

Author contributions

M.M. and T.S. conceived and designed the experiments. M.T., F.N., M.A., N.I., A.M.-S. and H.S. performed the experiments. M.M. conducted the project. M.M. and T.S. analysed data and wrote the paper.

Additional information

Supplementary Information accompanies this paper at http://www.nature.com/naturecommunications

Competing financial interests: The authors declare no competing financial interests.

Reprints and permission information is available online at http://npg.nature.com/reprintsandpermissions/

How to cite this article: Matsumoto, M. *et al.* Defined TLR3-specific adjuvant that induces NK and CTL activation without significant cytokine production *in vivo*. *Nat. Commun.* 6:6280 doi: 10.1038/ncomms7280 (2015).

OPEN ACCESS Freely available online

PLOS | ONE

System Vaccinology for the Evaluation of Influenza Vaccine Safety by Multiplex Gene Detection of Novel Biomarkers in a Preclinical Study and Batch Release Test

Takuo Mizukami[1], Haruka Momose[1], Madoka Kuramitsu[1], Kazuya Takizawa[1], Kumiko Araki[1], Keiko Furuhata[1], Ken J. Ishii[2,3], Isao Hamaguchi[1]*, Kazunari Yamaguchi[1]

1 Laboratory of Blood and Vaccine safety, Department of Safety Research on Blood and Biologicals, National Institute of Infectious Diseases, Tokyo, Japan, **2** Laboratory of Adjuvant Innovation, National Institute of Biomedical Innovation (NIBIO), Osaka, Japan, **3** Laboratory of Vaccine Science, WPI Immunology Frontier Research Center (WPI-IFREC), Osaka University, Osaka, Japan

Abstract

Vaccines are beneficial and universal tools to prevent infectious disease. Thus, safety of vaccines is strictly evaluated in the preclinical phase of trials and every vaccine batch must be tested by the National Control Laboratories according to the guidelines published by each country. Despite many vaccine production platforms and methods, animal testing for safety evaluation is unchanged thus far. We recently developed a systems biological approach to vaccine safety evaluation where identification of specific biomarkers in a rat pre-clinical study evaluated the safety of vaccines for pandemic H5N1 influenza including *Irf7, Lgals9, Lgalsbp3, Cxcl11, Timp1, Tap2, Psmb9, Psme1, Tapbp, C2, Csf1, Mx2, Zbp1, Ifrd1, Trafd1, Cxcl9, β2m, Npc1, Ngfr* and *Ifi47*. The current study evaluated whether these 20 biomarkers could evaluate the safety, batch-to-batch and manufacturer-to-manufacturer consistency of seasonal trivalent influenza vaccine using a multiplex gene detection system. When we evaluated the influenza HA vaccine (HAv) from four different manufactures, the biomarker analysis correlated to findings from conventional animal use tests, such as abnormal toxicity test. In addition, sensitivity of toxicity detection and differences in HAvs were higher and more accurate than with conventional methods. Despite a slight decrease in body weight caused by HAv from manufacturer B that was not statistically significant, our results suggest that HAv from manufacturer B is significantly different than the other HAvs tested with regard to *Lgals3bp, Tapbp, Lgals9, Irf7* and *C2* gene expression in rat lungs. Using the biomarkers confirmed in this study, we predicted batch-to-batch consistency and safety of influenza vaccines within 2 days compared with the conventional safety test, which takes longer. These biomarkers will facilitate the future development of new influenza vaccines and provide an opportunity to develop *in vitro* methods of evaluating batch-to-batch consistency and vaccine safety as an alternative to animal testing.

Citation: Mizukami T, Momose H, Kuramitsu M, Takizawa K, Araki K, et al. (2014) System Vaccinology for the Evaluation of Influenza Vaccine Safety by Multiplex Gene Detection of Novel Biomarkers in a Preclinical Study and Batch Release Test. PLoS ONE 9(7): e101835. doi:10.1371/journal.pone.0101835

Editor: Sang-Moo Kang, Georgia State University, United States of America

Received March 10, 2014; **Accepted** June 11, 2014; **Published** July 10, 2014

Data Availability: The authors confirm that all data underlying the findings are fully available without restriction. All data are included within the paper.

Funding: This work was supported by Grants-in-Aid from Ministry of Health, Labor, and Welfare of Japan (201132001 and 201208036, respectively). The funders had no role in study design, data collection and analysis, decision to publish, or preparation of the manuscript.

Competing Interests: The authors have declared that no competing interests exist.

* Email: 130hama@nih.go.jp

Introduction

Vaccination is a beneficial and universal tool to prevent infectious disease [1]. Because most vaccines are derived from inactivated virus, bacteria or toxoids, contamination by incomplete inactivation can cause serious adverse events. Thus, historically, the safety of vaccines is strictly regulated by law and each batch of vaccine must be tested by the National Control Laboratories according to the guidelines published in each country, *e.g.* the European Pharmacopeia, United States Pharmacopeia and World Health Organization guidelines [2]. After the diphtheria toxoid (DT) immunization incident in Japan in 1950 that caused the death of 68 children and illness in over 600 infants owing to contamination by incomplete inactivation of DT [3], the abnormal toxicity test (ATT) (also known as general safety test) was introduced to the Japanese guidelines. This stated that the minimum requirement of biological products (MRBP) and all inactivated vaccines and toxoids was mandatory safety evaluation by ATT and other specific toxicity tests.

Influenza vaccine is one of the most widely used commercially available vaccines worldwide for preventing seasonal influenza and its complications. Influenza virus vaccine is mainly produced using embryonated fertilized chicken eggs and inactivated with formaldehyde. Whole particle influenza virus vaccine [WPv] was first licensed as an influenza vaccine in the US in 1945 [4] and is still used in some countries. Although WPv contains all the components of the influenza virus and induces strong immunity in the vaccinated individual, a high incidence of adverse events, including local reactions at the site of injection and febrile illness, particularly among children have been reported [5,6]. Thus, most recent vaccines manufactured since the 1970s have been subvirion vaccines. The subvirion influenza HA vaccine [HAv] showed a marked reduction of pyrogenicity compared with WPv [7]. The trivalent influenza vaccine [TIV] is a recently developed subvirion

influenza vaccine with components selected and updated each year to protect against one of the three main groups of circulating influenza virus strains in humans. TIV may be administered every year. Vaccine adjuvant, e.g. alum, MF59 and AS03, was also used to enhance immunity in preparation for the H5N1 pandemic [8]. To improve immunogenicity and reduce toxicity in addition to batch-to-batch quality assurance of influenza vaccine, seed lot systems, recombinant DNA technology, as well as animal and insect cell culture inactivated vaccine production systems were introduced. Despite the increase in many vaccine production platforms, adjuvants, additives and vaccine types, safety evaluation tests in the preclinical phase and batch release have been unchanged in most countries, including in Japan.

We previously reported that improved ATT could evaluate and assure the batch-to-batch consistency of vaccines more strictly compared with conventional methods [9]. In addition, we recently introduced a system biological approach to vaccine safety evaluation and demonstrated that specific biomarkers could be used to evaluate batch-to-batch consistency and safety of vaccines to diphtheria-pertussis-tetanus (DPT) [10,11] and Japanese encephalitis virus (JEV) [12]. Most recently, we showed that a system biological approach could evaluate the safety of pandemic H5N1 influenza vaccine [13]. We found 20 biomarkers for the evaluation of batch-to-batch consistency and the safety of H5N1 vaccine compared with HAv.

In this study, we tested whether these biomarkers could evaluate batch-to-batch consistency and the safety of seasonal HAv, as well as adjuvanted whole virion-derived influenza vaccine, using a multiplex gene detection system. This method might facilitate the evaluation of batch-to-batch consistency of HAv and reduce the time required for batch release compared with conventional ATT. These biomarkers will help the future development of new *in vitro* methods to evaluate vaccine safety as an alternative to animal testing.

Materials and Methods

1. Animals and Ethics statement

Eight-week-old male Fischer (F334/N) rats weighing 160–200 g were obtained from SLC (Tokyo, Japan). All animals were housed in rooms maintained at 23±1°C, with 50±10% relative humidity, and 12-h light/dark cycles for at least 1 week prior to the test use. All animal experiments were performed according to the guidelines of the Institutional Animal Care and Use Committee of the National Institute of Infectious Diseases (NIID), Tokyo, Japan. The study was approved by the Institutional Animal Care and Use Committee of NIID.

2. Vaccines

The following vaccines were used in this study: (1) PDv: inactivated monovalent A/H5N1 whole-virion influenza vaccine (derived from NIBRG-14: A/Vietnam/1194/2004) adjuvanted with aluminum hydroxide, containing 30 μg HA/ml; (2) WPv: inactivated whole trivalent influenza vaccine (A/Newcaledonia/20/99 (H1N1), A/Hiroshima/52/2005 (H3N2), and B/Malaysia/2506/2004); HAV: trivalent HA influenza vaccine (A/Solomon Island/3/2006 (H1N1), A/Hiroshima/52/2005 (H3N2), and B/Malaysia/2506/2004), containing 30 μg HA/ml each strain. For evaluation of commercially distributed HAV in Japan, we used trivalent HA influenza vaccine (A/Solomon Island/3/2006 (H1N1), A/Hiroshima/52/2005 (H3N2) and B/Malaysia/2506/2004), containing 30 μg HA/ml per strain. PDv and WPv were produced, and manufactured by the Chemo-Sero-Therapeutic Research Institute, Kaketsuken (Kumamoto, Japan). Licensed and authorized HAvs were purchased from four different manufactur-

Table 1. Biomarkers to evaluate influenza vaccine safety.

Official Symbol	Official Full Name	Gene ID
Irf7	Interferon regulatory factor 7	293624
Lgals9	Lectin, galactoside-binding, soluble, 9	25476
Lgalsbp3	Lectin, galactoside-binding, soluble, 3 binding protein	245955
Cxcl11	Chemokine (C-X-C motif) ligand 11	305236
Timp1	TIMP metallopeptidase inhibitor 1	116510
Tap2	Transporter 2, ATP-binding cassette, sub-family B	24812
Psmb9	Proteasome (prosome, macropain) subunit, beta type, 9	24967
Psme1	Proteasome (prosome, macropain) activator subunit 1	29630
Tapbp	TAP binding protein (tapasin)	25217
C2	Complement component 2	24231
Csf1	Colony stimulating factor 1 (macrophage)	78965
Mx2	Myxovirus (influenza virus) resistance 2	286918
Zbp1	Z-DNA binding protein 1	171091
Ifrd1	Interferon-related developmental regulator 1	29596
Trafd1	TRAF type zinc finger domain containing 1	114635
Cxcl9	Chemokine (C-X-C motif) ligand 9	246759
β2m	Beta-2 microglobulin	24223
Npc1	Niemann-Pick disease, type C1	266732
Ngfr	Nerve growth factor receptor	24596
Ifi47	Interferon gamma inducible protein 47	246208

doi:10.1371/journal.pone.0101835.t001

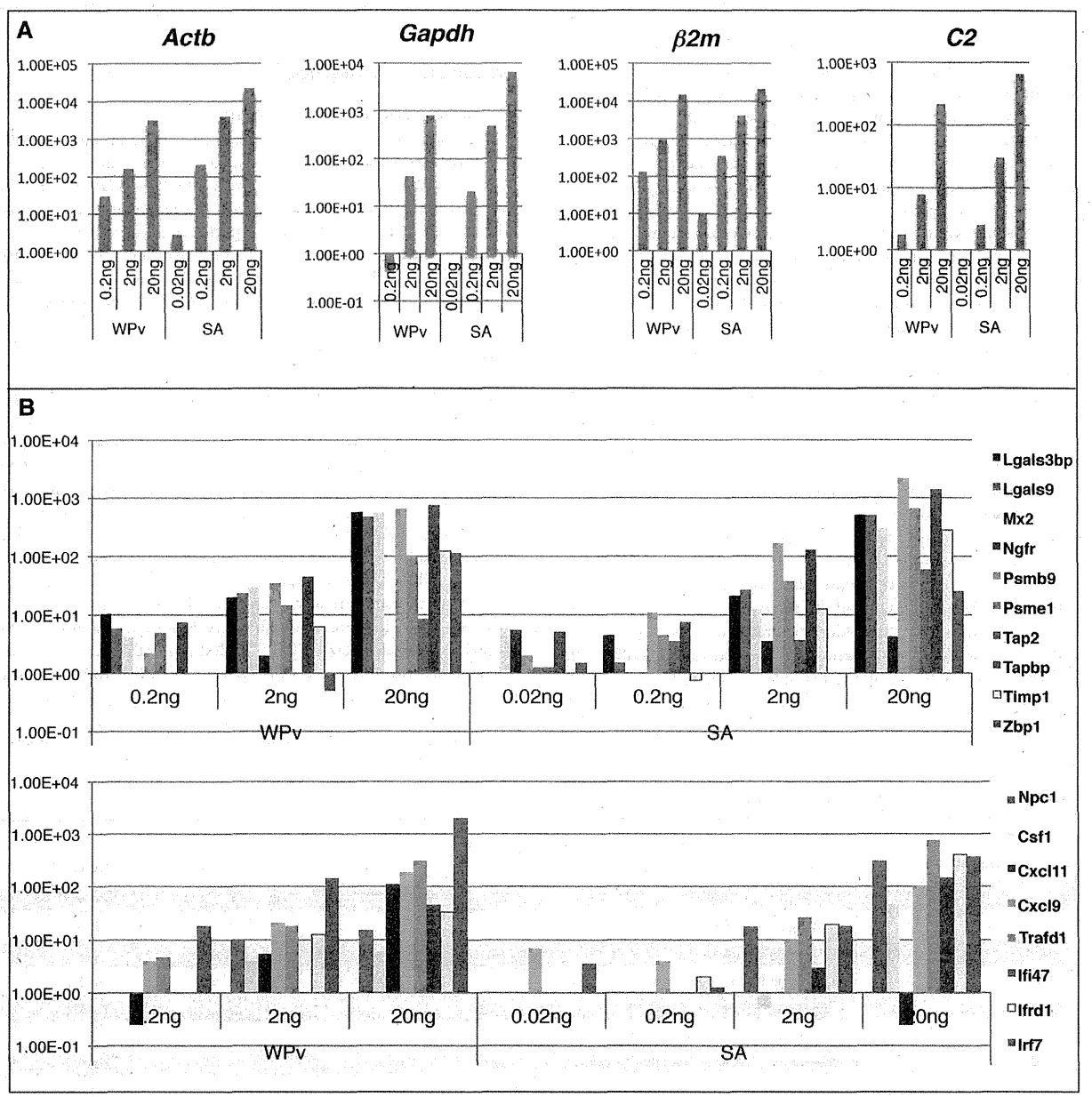

Figure 1. Optimization of QGP in influenza vaccine safety evaluation. A) Gene expression of *Actb*, *Gapdh*, *B2m* and *C2* and B) biomarkers, in 0.2, 2 and 20 ng RNA-containing samples from SA- and WPv-treated rat lungs. Relative expression levels of the *Gapdh* gene are indicated. SA: saline, WPv: Whole particle virion influenza vaccine.
doi:10.1371/journal.pone.0101835.g001

ers [HAv (Lot L03A) from Kaketsuken (Kumamoto), HAv (Lot 309) from Kitasato Institute (Saitama), HAv (Lot 343-A) from Denka Seiken Co., Ltd. (Tokyo), HAv (Lot HA082D) from Biken (Kagawa)] in Japan. All vaccines complied with the MRBP in Japan. HAv used in this study was tested and authorized by NCL (National Control Laboratory) for distribution in Japan.

3. Abnormal toxicity test

ATT was performed according to the MRBP [http://www.nih.go.jp/niid/en/mrbp-e.html] using rats with a slight modification. Each 5 ml of vaccine was intra-peritoneally (*i.p.*) injected into rats. Five milliliters of saline (SA) (Otsuka normal saline; Otsuka Pharmaceutical Factory Inc., Naruto, Tokushima, Japan) was *i.p.* injected as a control. One day after the injection, rat body weight was measured and peripheral blood was collected. The number of white blood cells was counted with a hemocytometer (Nihon Kohden, Japan).

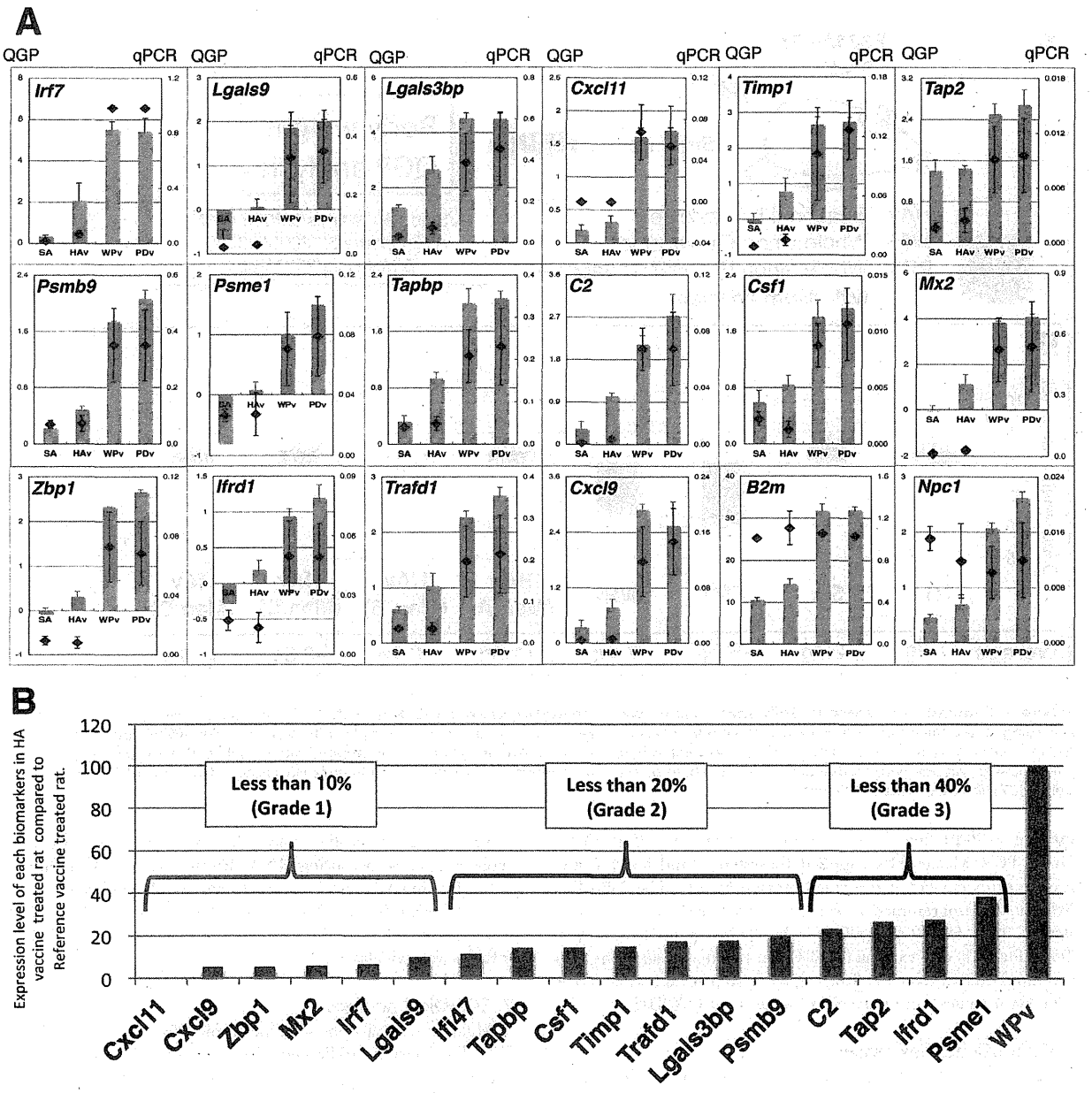

Figure 2. Validation of QGP with real-time PCR methods. A) GQP result was validated with real-time PCR methods. Bar graph indicates the real-time PCR results and dot blot indicates QGP results. B) Biomarkers were classified into three grades according to the relative expression level compared with WPv-treated rats.
doi:10.1371/journal.pone.0101835.g002

4. RNA preparation

One day after injection, rats were sacrificed to obtain whole lung tissues. Organs were immediately frozen in liquid nitrogen for storage. Thawed tissue was homogenized and mixed with an Isogen reagent (Nippon Gene, Tokyo, Japan). Total RNA was prepared from the lysate in accordance with the manufacturer's instructions. Poly (A)+ RNA was prepared from total RNA with a Poly (A) Purist Kit (Ambion, Austin, TX), according to the manufacturer's instructions.

5. Quantitative RT-PCR analysis

Poly (A)+ RNA was used to synthesize first-strand cDNA using a First-strand cDNA Synthesis Kit (Life Science Inc., St. Petersburg, FL), according to the manufacturer's instructions. Expression levels of biomarkers (**Table 1**) were analyzed by real-time polymerase chain reaction (PCR) using a 7500 Fast Real-Time PCR System (Applied Biosystems, Foster City, CA) with 7500 Fast System SDS Software Version 1.3. cDNA was amplified for real-time PCR using SYBR Green I (Molecular Probes Inc.) to detect the PCR products. One microliter of 6-fold diluted cDNA was

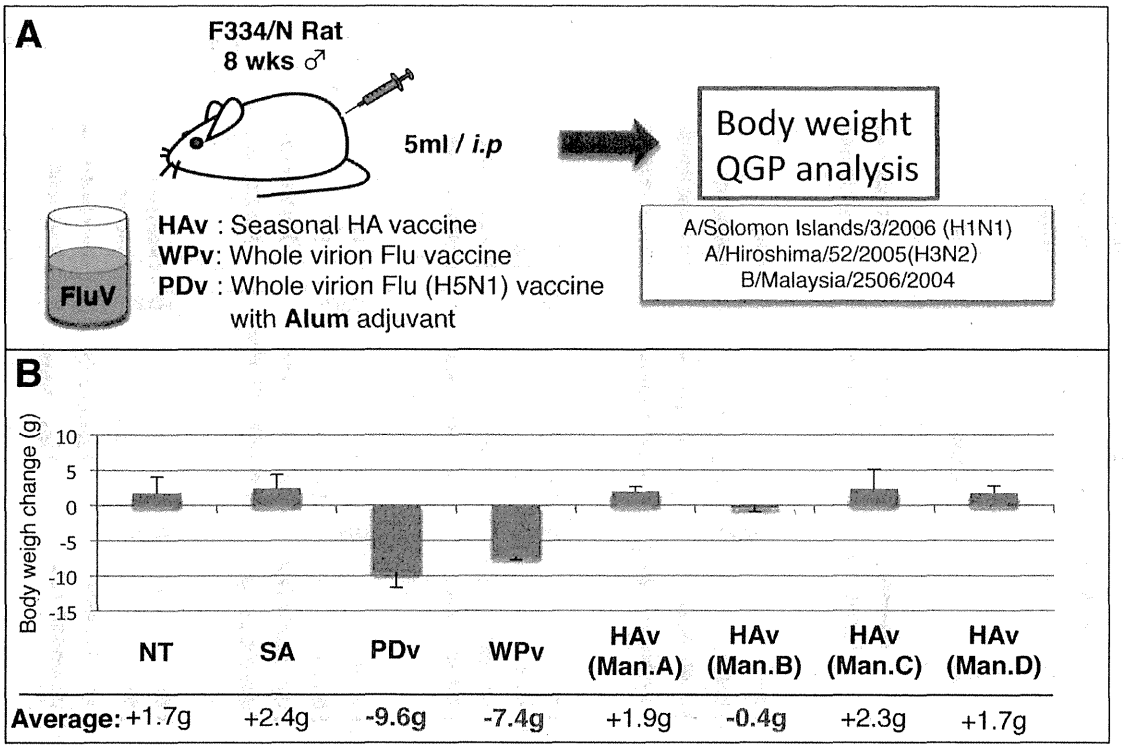

Figure 3. Evaluation of seasonal influenza vaccine with conventional animal safety test. A) The abnormal toxicity test was performed according to the Minimum Requirements of Biological Products. Each 5 ml vaccine was *i.p.* injected into rats, the body weight measured and lung tissues collected at day 1 after injection. B) Body weight change at day 1 after injection. NT: nontreated rat, SA: saline, PDv: pandemic H5N1 whole virion-derived vaccine with alum adjuvant, WPv: whole particle virion influenza vaccine, HAv: influenza HA vaccine, Man: manufacturer.
doi:10.1371/journal.pone.0101835.g003

used in a 20-μl final volume reaction containing 10 μl SYBR Green PCR Master Mix (Applied Biosystems), and forward and reverse primers were as described previously [13]. The 7500 Fast System was programmed to run an initial polymerase activation step at 95°C for 10 min followed by 40 cycles of denaturation (95°C for 15 s) and extension (60°C for 1 min). Product synthesis was monitored at the end of the extension step of each cycle. Gene expression values were normalized against rat GAPDH.

6. QuantiGene Plex assays

QuantiGene Plex (QGP) assays were performed according to the QuantiGene Plex Reagent System instructions (Panomics Inc., Fremont, CA), as described previously [11]. Briefly, 10 μl of starting poly (A)+RNA (50 ng) was incubated for 10 min at 65°C, then mixed with 33.3 μl of lysis mixture, 40 μl of capture buffer, 2 μl of capture beads, and 2 μl of the target gene-specific probe set. Probe sets were heated for 5 min prior to use. Each sample mixture was then dispensed into an individual well of a capture plate, sealed with foil tape and incubated at 54°C for 16–20 h. The hybridization mixture was transferred to a filter plate, and the wells were washed three times with 200 μl of wash buffer. Signals for the bound target mRNA were developed by sequential hybridization with branched DNA (bDNA) amplifier, and biotin-conjugated label probe, at 48°C for 1 h each. Two washes with wash buffer were used to remove unbound material after each hybridization step. Streptavidin-conjugated phycoerythrin was added to the wells and incubated at room temperature for 30 min. The luminescence of each well was measured using a Luminex 100 microtiter plate luminometer (Luminex). Two replicate assays measuring RNA directly (independent sampling $n = 6$ for mRNA, $n = 3–5$ for lysate) were performed for all described experiments. The 20 target genes and GAPDH mRNA were quantified, and the ratio of the target genes to GAPDH mRNA was calculated.

7. Statistical analysis

Multiple comparisons were performed for SA, PDv, WPv and HA. To determine differences between manufacturers, multiple comparisons were performed for SA and HA from manufacturers A, B, C and D. Statistical analysis was performed in GraphPad Prism 6 (GraphPad Software, La Jolla, CA) using an ordinary one-way analysis of variance test followed by a Tukey multiple comparison test.

Results

Optimization of multiple gene detection system, QuantiGene Plex, for safety evaluation of the influenza vaccine

We previously reported that 20 selected genes (**Table 1**), from 76 differentially expressed genes in adsorbed PDv-treated rats, could be used as biomarkers to evaluate H5N1 influenza vaccine safety compared with other types of influenza vaccine using conventional real-time PCR [13]. To establish faster and more convenient methods to detect these biomarkers in one-step as a new vaccine safety test, we used QuantiGene Plex (QGP)

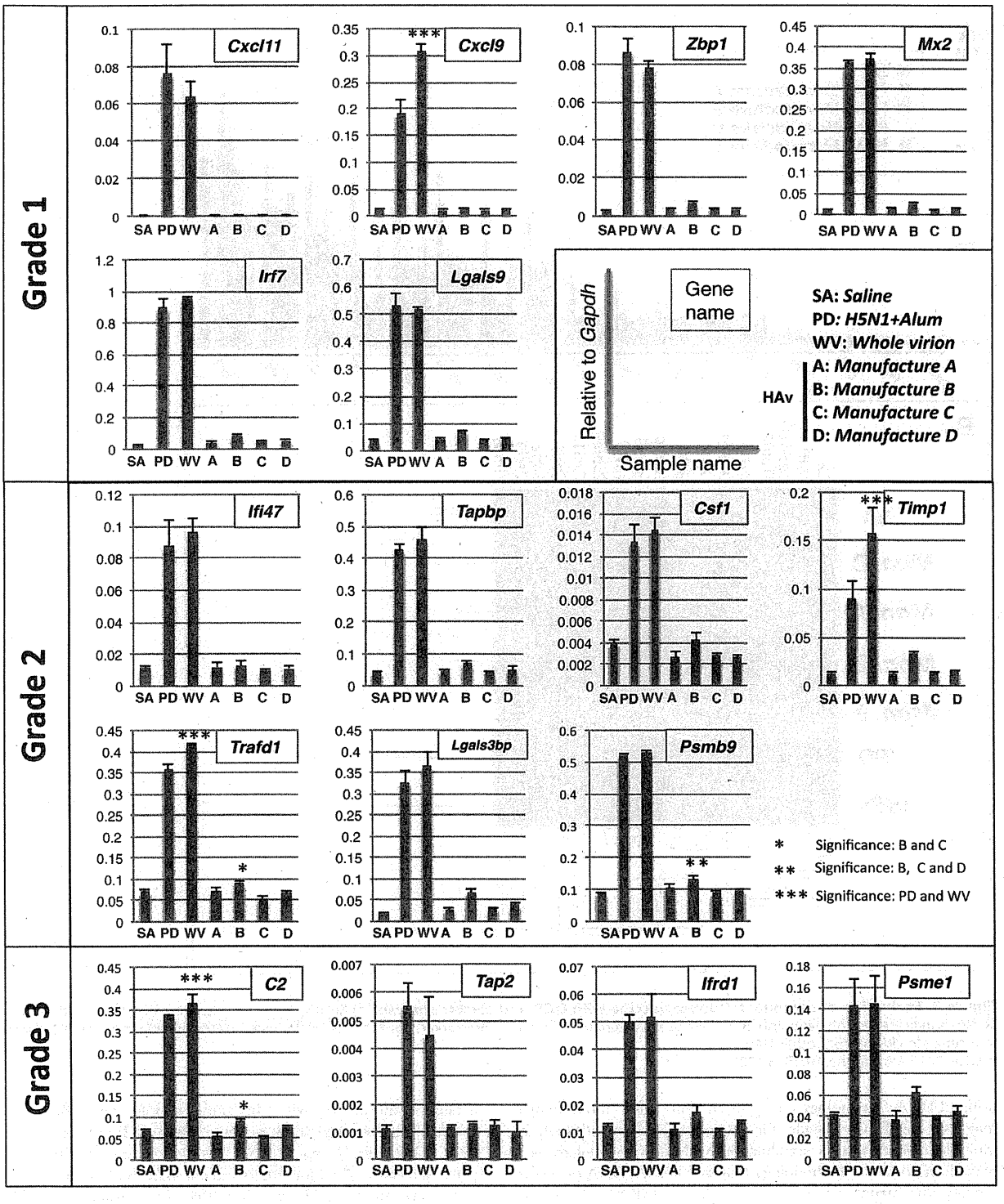

Figure 4. Evaluation of seasonal influenza vaccine with QGP. The relative gene expression levels of the *Gapdh* gene are indicated in each column (grades 1, 2 and 3, respectively). *Significant difference between B and C. **Significant difference between B, C and D, ***Significant difference between PD and WPv.
doi:10.1371/journal.pone.0101835.g004

technology (Panomics Inc., Fremont, CA). We designed a custom QGP 2.0 assay to enable the measurement of expression levels of identified biomarkers. The Panomics QGP 2.0 assays provided quantitative measurements of 3 to 80 target RNAs per well by

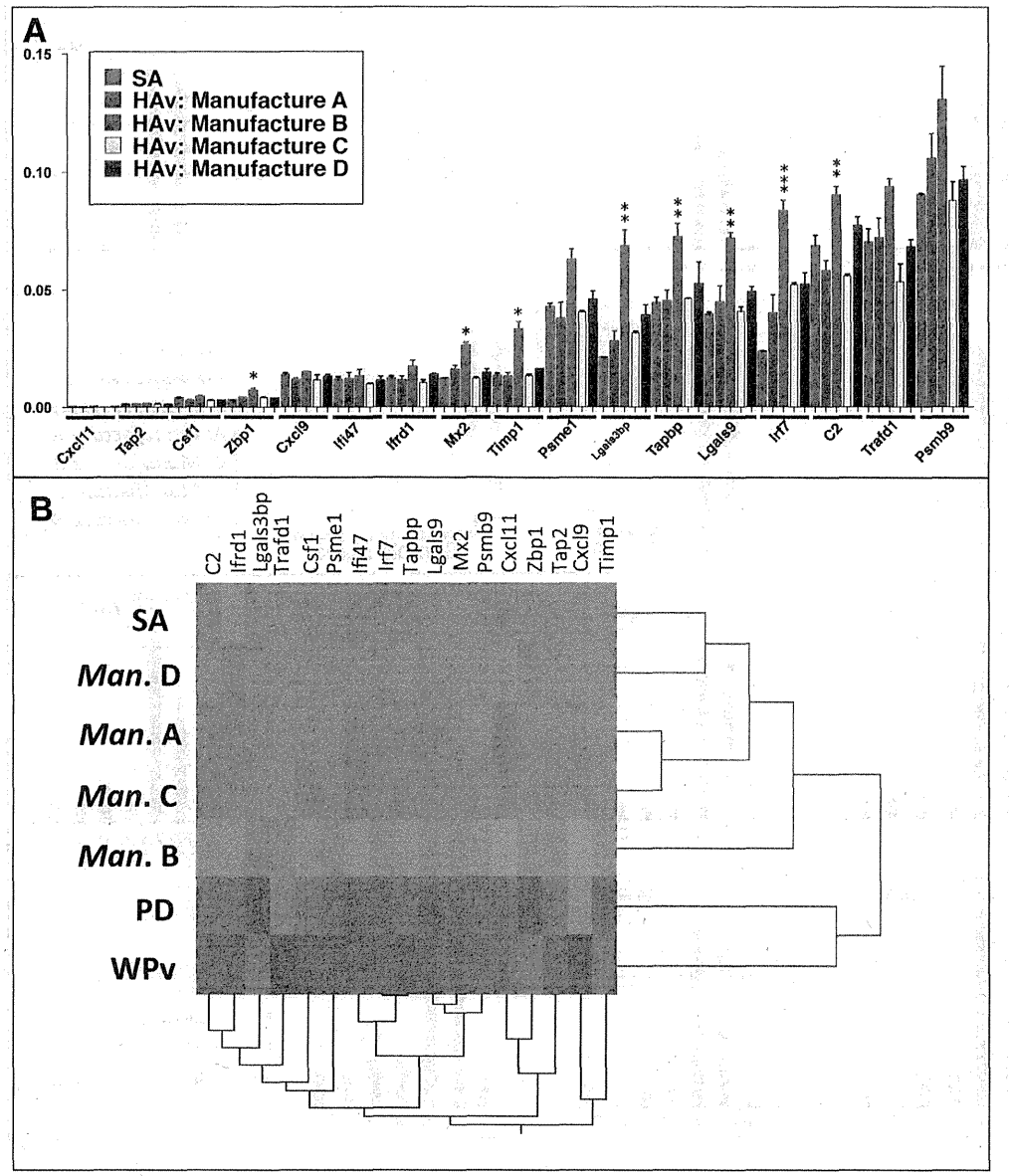

Figure 5. Evaluation of seasonal influenza vaccine with QGP and cluster analysis. A) Relative gene expression in HAv-treated rat lungs to *Gapdh* is indicated in the bar graph. B) Hierarchical clustering analysis with biomarkers could predict differences in HAv manufacturers as B is located in a separate cluster from other HAvs.
doi:10.1371/journal.pone.0101835.g005

using bDNA technology in conjunction with multi-analyte magnetic beads to provide the detection and quantitation of multiple mRNA targets simultaneously. bDNA technology is a hybridization-based methodology that uses labeled DNA probes to amplify the signal rather than the target mRNA. Here, we produced probes for 20 genes and two control genes (*Actb* and *Gapdh*) for the one-step detection and quantification of these biomarkers. To check the sensitivity of probes and dynamic range of our biomarkers, we prepared 0.02, 0.2, 2 and 20 ng total RNA samples from WPv and SA-treated rat lungs and performed QGP analysis. Two control genes and two biomarkers (*β2m* and *C2*) reacted in a dose-dependent manner (**Figure 1A**). We re-evaluated all probes with the same sample. Each biomarker reacted in a dose-dependent manner (**Figure 1B**) except *Ngfr* and *Npc1*. Therefore, 20 ng of RNA sample was used for multiplex gene detection. All biomarkers except *β2m* reacted in a dose-dependent manner. *β2m* was saturated when using 20 ng RNA sample; thus *β2m* could not be used for QGP analysis.

Validation of QGP with real-time PCR

To validate QGP, we performed real-time PCR analysis using the same samples. As a result, most biomarker gene expression data from the QGP correlated with the real-time PCR result except for *β2m*, *Npc1* (Figure 2) and *Ngfr* (data not shown). Finally,

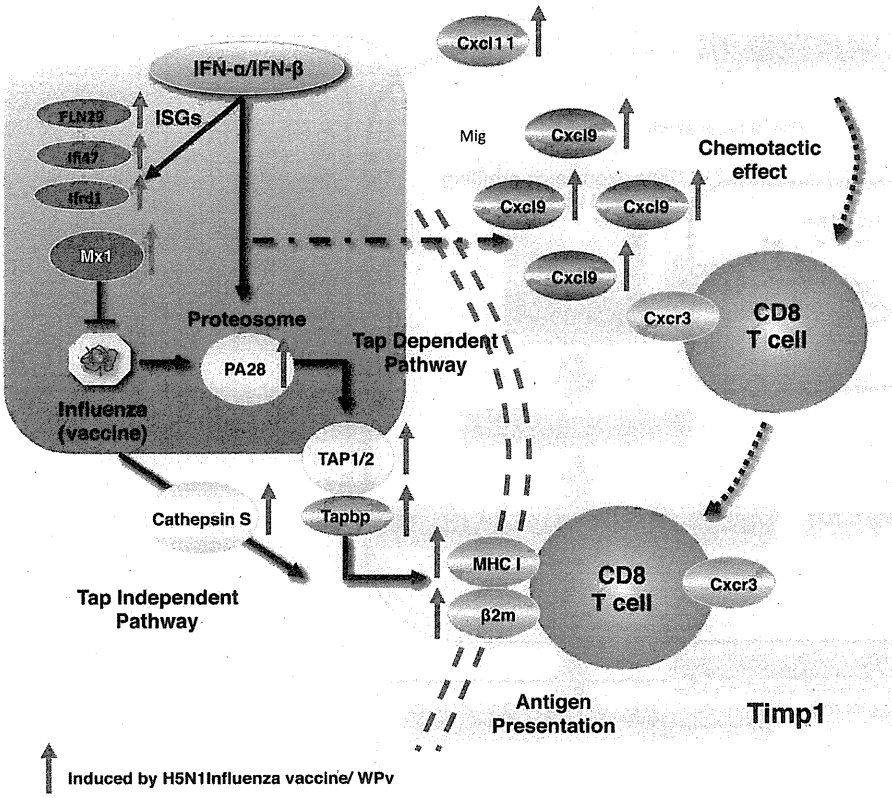

Figure 6. Summary of biomarker studies. Biomarkers used in this study were strongly correlated with immune responses after influenza infection.
doi:10.1371/journal.pone.0101835.g006

17 genes were selected as the multiplex detection biomarker set. We next determined the relative biomarker expression levels in HAv-treated rat lungs compared with WPv used as a reference toxicity vaccine in the leukopenic toxicity test (LTT) in Japan. We classified *Cxcl11*, *Cxcl9*, *Zbp1*, *Mx2*, *Irf7* and *Lgals9* as a "Grade 1" gene set where relative expression levels in HAv compared with WPv were less than 10%. Likewise, we classified *Ifi47*, *Tapbp*, *Csf1*, *Timp1*, *Trafd1*, *Lgals3bp* and *Psmb9* as a "Grade 2" gene set where relative expression levels were less than 20% and *C2*, *Tap2*, *Ifrd1* and *Psme1* as a "Grade 3" gene set where relative expression levels were less than 40% in HAv compared with WPv. In Japan, it is acceptable for leukopenic toxicity levels of HAv to be not more than 20% of WPv by LTT. We applied LTT criteria for selecting and subdividing these biomarkers into three grades with expression levels below 20% of WPv and others.

Evaluation of HAv safety in Japan using ATT and QGP

To evaluate the toxicity of seasonal HAv using biomarkers, we purchased market authorized seasonal influenza vaccines distributed in Japan from four different manufacturers (Kaketsuken, Denka Seiken, Kitasato, and Biken). Although the vaccines have been evaluated and passed ATT by the NCL according to the Japanese guidelines for MRBP, the reactogenicity of the vaccine to animals (rats, mice and guinea pigs) was varied. To evaluate these differences, we performed ATT and checked the body weight changes of rats after *i.p.* injection of each HAv (Figure 3A). Although treatment with PDv or WPv (toxic reference whole virion-derived vaccines) significantly decreased the body weight of rats, HAvs from three different manufacturers had no effect on body weight. HAv from manufacture B reduced the body weight of rats at day 1 (Figure 3B). However, there was no significant difference in rat body weight change for the other HAvs; thus HAv from manufacturer B might be slightly different, when comparing the mean body weight at day 1. In addition, there was no significant difference in leukocyte numbers following administration of HAv from the four manufacturers (data not shown). To evaluate the differences of each HAv, we next performed multiplex biomarker detection by QGP. No biomarkers were significantly up-regulated in HAv-treated rats compared with controls (Figure 4) except for *Psmb9*. Furthermore, *Psmb9* expression was significantly up-regulated following administration of HAv from manufacturer B compared with the control SA-treated and HAvs from the other manufacturers. The expression levels of *C2* and *Trafd1* were also significantly up-regulated in the HAv from manufacturer B compared with the HAv from manufacturer C.

Biomarkers to evaluate safety of adjuvanted influenza vaccine

Both PDv and WPv contain the whole virion influenza vaccine and alum adjuvant is only added to PDv to enhance its immunogenicity. There was no difference in body weight change between WPv- and PDv-treated rats (Figure 3B). However, among the 17 biomarkers, the expression level of three genes, *Cxcl9*, *Timp1* and *Trafd1* in PDv-treated rats were significantly decreased compared with WPv-treated rats (Figure 4). Thus, these biomarkers could potentially evaluate the aluminum adjuvant effect.

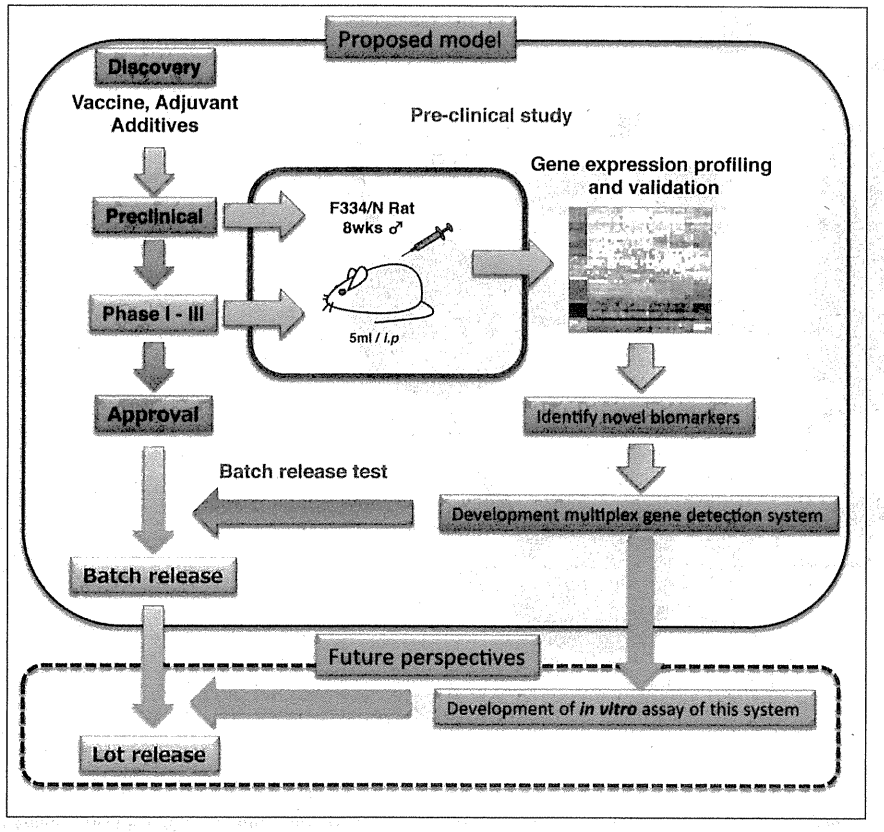

Figure 7. Application of the system biological approach for influenza vaccine development. Proposed model of future influenza vaccine development and establishment of preclinical studies and batch release testing. Acquisition of transcriptome data at the preclinical and clinical phase is useful for future batch release testing and the prediction of vaccine efficacy and toxicity.
doi:10.1371/journal.pone.0101835.g007

Cluster analysis of QGP data predicts influenza vaccine safety

Conventional animal tests such as ATT and LTT have been performed in Japan for the evaluation of influenza vaccine safety and toxicity. Despite applying these tests that evaluate whole virion-derived influenza vaccine from HAv, it is difficult to distinguish statistically between different HAvs if they do not have comparable toxicity greater than 20–50% to WPv. According to the body weight change observed with ATT, we speculated that HAv from manufacturer B was slightly different than the others tested (Figure 3B), although this was not statistically significant. However, when biomarkers were used with QGP to evaluate HAvs, we could distinguish the HAv from manufacturer B compared with those from other manufacturers. When we focused on biomarker expression among the HAv-treated rat lungs, the expression levels of *Zbp1*, *MX2*, *Timp1*, *Lgals3bp*, *Tapbp*, *Lgals9*, *Irf7* and *C2* were significantly up-regulated in rat lungs treated with HAvs from manufacturer B (Figure 5A). In addition, cluster analysis with the biomarkers predicted differences in HAvs as the vaccine from manufacturer B was located in a separate cluster from the other HAvs. Thus, these biomarkers can evaluate batch-to-batch and manufacturer-to-manufacturer differences in HAvs (Figure 5B).

Discussion

Vaccine safety is critical in the process of vaccine development and universal vaccination. Several vaccines were stopped owing to safety concerns, including severe side effects, after they had received marketing authorization and licensing, even when they were effective [14]. To ensure the safety of vaccines, the preclinical phase in the development of vaccines and the batch release system after marketing authorization is critical. However, the guidelines for nonclinical assessment of vaccines and batch release tests only focus on the evaluation of vaccine efficacy and immunogenicity in animal models, quality control testing programs and toxicology testing in relevant animal models [15]. These guidelines do not include scientific research for identifying the potential toxicities of the vaccines, adjuvants and additives.

We have demonstrated the advantage of a system biological approach using several vaccines authorized in Japan, *e.g.* DPT, JEV and Influenza vaccine including H5N1 pandemic influenza vaccine [10–13]. We successfully identified several biomarkers to evaluate DPT, JEV and influenza vaccine toxicity. In this study, we demonstrate that the biomarkers used to evaluate H5N1 pandemic influenza vaccine could also be used to evaluate the batch-to-batch consistency and the safety of HAvs. In addition, they can be used to evaluate manufacturer-to-manufacturer differences using the multiplex gene detection system. The biomarker analysis correlated to findings from conventional

animal use tests, such as ATT. In addition, sensitivity of toxicity detection and differences in HAvs was higher and more accurate than with conventional methods. Despite all the HAvs evaluated in this study meeting MRBP criteria and passing NCL, our results suggest that HAv from manufacturer B is slightly different than the HAvs according to *Lgals3bp*, *Tapbp*, *Lgals9*, *Irf7* and *C2* gene expression. Among the official vaccine adverse event information provided by the Japanese authorities, there is no reported evidence that the adverse event rate was increased or that severe adverse events were observed caused by HAv from manufacturer B. It is still unknown what factors (additives, formalin content, protein content) induce these biomarkers in the HAv from manufacturer B. Further studies are needed to determine whether our biomarkers could predict the toxicity of influenza vaccine by using different formulations of HAv. Using biomarkers from any grade characterized in this study, we could also predict the safety of influenza vaccines within 2 days whereas the conventional animal use safety test, ATT requires 7 days for evaluating batch-to-batch consistency and vaccine safety. Further studies are needed to determine how these biomarkers can be used to evaluate the safety of HAv. To set the percent limit of up-regulation of each biomarker, it might be helpful to compare another conventional test such as LTT [[http://www.nih.go.jp/niid/en/mrbp-e.html]] as well as a comparison of failed batches of HAv. LTT evaluates the peripheral leukocyte number reduction rate compared with WPv. In general, WPv induces a strong loss of peripheral leukocyte numbers 16 hours after WPv administration in mice [9 and 28]. The test criteria of LTT is that the loss of leukocyte numbers in test samples must be no greater than 20% compared with a reference toxic vaccine such as WPv or less than 50% of SA-treated mice. These criteria may be applicable to set our biomarker expression limit. Further validation is required to set the limit the gene expression level.

Influenza is a socially important infectious disease that causes seasonal flu outbreaks worldwide and has a pandemic status [16]. Correspondingly, many types of influenza vaccine (cell derived, recombinant derived, live attenuated and inactivated influenza vaccine), have been developed to ensure efficacy and reduce toxicity [17]. While some adjuvants have been developed and used to amplify vaccine efficacy [8], the safety of adjuvants is still of concern. Recently, several adjuvants (squalene-based MF59 and AS03) developed and licensed for use only in pandemic influenza vaccines were under investigation for the occurrence of narcolepsy in vaccinated children in European countries [18]. Conventional safety tests could be used to evaluate the safety of these vaccines [19], but it is still difficult to predict the safety and toxicity of influenza vaccines, adjuvants and additives [20]. We demonstrated that usage of system biological approaches to evaluate safety might revolutionize vaccine testing methods [21]. Most of the previously identified biomarkers were up-regulated and correlated with influenza infection, interferon responses, antigen presentation and antibody production (Figure 6). In addition, we found that several biomarkers, *Cxcl9*, *Trafd1*, and *C2* were candidates for evaluating differences between alum-adjuvanted influenza vaccines and nonadjuvanted vaccines. Further studies, using several adjuvants, are needed to confirm the feasibility of these biomarkers in evaluating adjuvant safety.

In addition to whole transcriptome analysis of vaccinated animals, recent advances in genome research enabled the acquisition of whole transcriptional data from vaccinated individuals and identification of gene expression after immunization with vaccines to yellow fever, measles, tularemia and tuberculosis [22]. With a focus on the influenza vaccine, Bucasas et al. reported a 494 gene set, including biomarkers identified in our previous study (*MX1*, *IRF7*) that strongly correlated with antibody responses in humans [23]. Wei et al. reported gene expression differences between HAv and live attenuated influenza vaccine. They identified 265 differentially expressed genes, including our previously identified biomarkers, *IRF7*, *MX1*, *MX2*, *OAS1* and *ZBP1* [24].

Recently, Nakaya and Pulendran reported a system biological approach, termed systems vaccinology [25], which was used to predict immunogenicity and provide new mechanistic insights regarding influenza vaccination. They also reported several gene sets that predicted influenza vaccine immunogenicity, including our previously identified biomarkers, *MX1*, *MX2*, *OAS1* and *IRF7* [26]. More recently, Franco et al. reported 20 genes, including our biomarkers, *TAP2* and *OAS1*, which correlated with antibody responses, using integrative genomic analysis [27]. All these reports suggest that using animal models is still useful if biomarkers are up-regulated in vaccinated individuals and can reveal the role of biomarkers in immune responses and vaccination toxicity. Thus, in the preclinical and clinical phase, the acquisition of transcriptome data from both vaccinated individuals and animals, and a comparison of these data will be helpful for future vaccine development and batch release testing (Figure 7).

Taken together, system biological approaches to identify vaccine toxicity using whole genome transcriptome methods will improve vaccine development in preclinical and clinical phases if more data are generated from successfully vaccinated individuals and those with side effects. It is still unclear whether and how these factors determine immunogenicity and toxicity. Further studies are required to identify and reveal the mechanisms underlying vaccination in humans and in animal models, including nonhuman primates.

Acknowledgments

The authors acknowledge Dr. Shinya Watanabe, Junichi-Imai for technical support of the initial transcriptome analysis after influenza vaccination of rats. The authors wish to thank Dr. Hiroshi Yamada for his advice on performing toxicogenomic studies.

Author Contributions

Conceived and designed the experiments: TM. Performed the experiments: TM HM MK KT. Analyzed the data: TM HM KJI IH KY. Contributed reagents/materials/analysis tools: TM HM MK KT KA KF KJI. Wrote the paper: TM.

References

1. Plotkin SL, Plotkin SA (2012) A short history of vaccination. General aspects of vaccination. In: Plotkin SA, Orenstein WA, Offit PA, editors. 6th edition Vaccines. Philadelphia: Saunders Elsevier. 1–13.
2. Baylor NW, Marshall VB (2012) Regulation and testing of vaccines. In: Plotkin SA, Orenstein WA, Offit PA, editors. 6th edition Vaccines. Philadelphia: Saunders Elsevier. 1427–1446.
3. Kurokawa M, Murata R (1961) On the Toxicity of the Toxoid Preparation Responsible for the Kyoto Catastrophe in 1948. Jpn J Med Sci Biol 14: 249–256.
4. Wood JM, Williams MS (1998) History of inactivated influenza vaccines. In: Nicholson KG, Webster RG, Hay AJ, editors. Textbook of influenza. Oxford: Blackwell Science. 317–323.
5. Nicholson KG, Tyrrell DA, Harrison P, Potter CW, Jennings R, et al. (1979) Clinical studies of monovalent inactivated whole virus and subunit A/USSR/77 (H1N1) vaccine: Serological responses and clinical reactions. J Biol Stand 7: 123–136.
6. Wright PF, Thompson J, Vaughn WK, Folland DS, Sell SH, et al. (1977) Trials of influenza A/New Jersey/76 virus vaccine in normal children: an overview of age-related antigenicity and reactogenicity. J Infect Dis 136: S731–S741.

7. Couch RB, Keitel WA, Cate TR (1997) Improvement of inactivated influenza virus vaccines. J Infect Dis. 176 Suppl 1: S38–44.
8. Even-Or O, Samira S, Ellis R, Kedar E, Barenholz Y (2013) Adjuvanted influenza vaccines. Expert Rev Vaccines. 12: 1095–1108.
9. Mizukami T, Masumi A, Momose H, Kuramitsu M, Takizawa K, et al. (2009) An improved abnormal toxicity test by using reference vaccine-specific body weight curves and histopathological data for monitoring vaccine quality and safety in Japan. Biologicals. 37: 8–17.
10. Hamaguchi I, Imai J, Momose H, Kawamura M, Mizukami T, et al. (2007) Two vaccine toxicity-related genes Agp and Hpx could prove useful for pertussis vaccine safety control. Vaccine. 25: 3355–3364.
11. Hamaguchi I, Imai J, Momose H, Kawamura M, Mizukami T, et al. (2008) Application of quantitative gene expression analysis for pertussis vaccine safety control. Vaccine. 26: 4686–4696.
12. Momose H, Imai J, Hamaguchi I, Kawamura M, Mizukami T, et al. (2010) Induction of indistinguishable gene expression patterns in rats by Vero cell-derived and mouse brain-derived Japanese encephalitis vaccines. Jpn J Infect Dis. 63: 25–30.
13. Mizukami T, Imai J, Hamaguchi I, Kawamura M, Momose H, et al. (2008) Application of DNA microarray technology to influenza A/Vietnam/1194/2004 (H5N1) vaccine safety evaluation. Vaccine. 26: 2270–2283.
14. Offit PA, Stefano FD (2012) Vaccine safety. In: Plotkin SA, Orenstein WA, Offit PA, editors. 6th edition Vaccines. Philadelphia: Saunders Elsevier. 1464–1480.
15. Wolf JJ, Kaplanski CV, Lebron JA (2010) Nonclinical safety assessment of vaccines and adjuvants. Methods Mol Biol. 626: 29–40.
16. WHO (2013) Pandemic Influenza Risk Management, WHO Interim Guidance. Available: http://www.who.int/influenza/preparedness/pandemic/GIP_PandemicInfluenzaRiskManagementInterimGuidance_Jun2013.pdf. Accessed 2014 June 18.
17. Wong SS, Webby RJ (2013) Traditional and new influenza vaccines. Clin Microbiol Rev. 26: 476–492.
18. Ahmed SS, Schur PH, Macdonald NE, Steinman L (2014). Narcolepsy, 2009 A (H1N1) pandemic influenza, and pandemic influenza vaccinations: What is known and unknown about the neurological disorder, the role for autoimmunity, and vaccine adjuvants. J Autoimmun. 50: 1–11.
19. Brennan FR1, Dougan G (2005) Non-clinical safety evaluation of novel vaccines and adjuvants: new products, new strategies. Vaccine. 23: 3210–3222.
20. Verdier F, Morgan L (2001) Predictive value of pre-clinical work for vaccine safety assessment. Vaccine. 20 Suppl 1: S21–23.
21. Momose H, Mizukami T, Ochiai M, Hamaguchi I, Yamaguchi K (2010) A new method for the evaluation of vaccine safety based on comprehensive gene expression analysis. J Biomed Biotechnol. 2010: 361841.
22. Wang IM, Bett AJ, Cristescu R, Loboda A, ter Meulen J (2012) Transcriptional profiling of vaccine-induced immune responses in humans and non-human primates. Microb Biotechnol. 5: 177–187.
23. Bucasas KL, Franco LM, Shaw CA, Bray MS, Wells JM, et al. (2011) Early patterns of gene expression correlate with the humoral immune response to influenza vaccination in humans. J Infect Dis. 203: 921–929.
24. Zhu W, Higgs BW, Morehouse C, Streicher K, Ambrose CS, et al. (2010) A whole genome transcriptional analysis of the early immune response induced by live attenuated and inactivated influenza vaccines in young children. Vaccine. 28: 2865–2876.
25. Pulendran B, Li S, Nakaya HI (2010) Systems vaccinology. Immunity. 33: 516–529.
26. Nakaya HI, Wrammert J, Lee EK, Racioppi L, Marie-Kunze S, et al. (2011) Systems biology of vaccination for seasonal influenza in humans. Nat Immunol. 12: 786–795.
27. Franco LM, Bucasas KL, Wells JM, Niño D, Wang X, et al. (2013) Integrative genomic analysis of the human immune response to influenza vaccination. Elife. 2: e00299.
28. Ato M, Takahashi Y, Fujii H, Hashimoto S, Kaji T, et al. (2013) Influenza A whole virion vaccine induces a rapid reduction of peripheral blood leukocytes via interferon-α-dependent apoptosis. Vaccine. 31: 2184–2190.